# Amorphous-Carbon/Si Heterojunction device for Room Temperature $NH_3$ Sensing and Development of Readout Circuit for Chemiresistive Sensor

Eliganti Venkatesh
(EE16MTECH11004)

A Dissertation Submitted to
Indian Institute of Technology Hyderabad
In Partial Fulfillment of the Requirements for
The Degree of Master of Technology/ Doctor of Philosophy

Under esteemed Guidance of
Prof. Shiv Govind Singh

भारतीय प्रौद्योगिकी संस्थान हैदराबाद
Indian Institute of Technology Hyderabad

Department of Electrical Engineering
June, 2018

## Declaration

I declare that this written submission represents my ideas in my own words, and where others' ideas or words have been included, I have adequately cited and referenced the original sources. I also declare that I have adhered to all principles of academic honesty and integrity and have not misrepresented or fabricated or falsified any idea/data/fact/source in my submission. I understand that any violation of the above will be a cause for disciplinary action by the Institute and can also evoke penal action from the sources that have thus not been properly cited, or from whom proper permission has not been taken when needed.

Eliganti Venkatesh
EE16MTECH11004

## Approval Sheet

This thesis entitled "Amorphous-Carbon/Si heterojunction device for room temperature $NH_3$ Sensing and Development of Readout Circuit for Chemiresistive Sensor" by Eliganti Venkatesh is approved for the degree of Master of Technology from IIT Hyderabad.

Dr. Shiv Govind Singh
Professor, Dept of Electrical Engineering.,IITH
Adviser

Dr. Gajendranath Chaudhury
Assistant Professor, Dept of Electrical Engineering.,IITH
Examiner

Dr.Soumya Jana
Associate Professor,Dept of Electrical Engineering.,IITH
Chairman

# Acknowledgements

I sincerely thank my supervisors Prof. Shiv Govind Singh and Dr. Gajendranath Chowdary for their guidance and moral support throughout the project. I acknowledge the fabrication facilities provided by Nano X lab, Electrical Department, IIT Hyderabad for the successful completion of this project.

I would like to extend my thanks to each and every person from Nano X lab Satish sir, Jose sir, Santosh sir, Hemanth, Supraja. I heartfully thank Suryasnata Tripathy for his continuous support throughout the project and also I would like to acknowledge his contribution in fabrication and characterization part of the device. Without his support I would not be able to complete this project. I would like to acknowledge all the characterization facilities provided by Electrical, Physics departments of IIT Hyderabad.

I would like to express my deepest sense of gratitude to my parents, brother for their continuous support and encouragement.

- Eliganti Venkatesh

Dedicated to

My Parents & Teachers

# Abstract

Classical metal oxide gas sensors are used to be operated at relatively high temperatures to achieve good sensitivity. So there is a strong need to develop a gas sensing platform that provides either low temperature or room temperature sensing, so as to reduce the power consumption. Keeping this in mind, in this work, we have proposed and fabricated an amorphous-Carbon/Silicon (a-C/Si) heterojunction based room temperature ammonia gas sensor. We have optimized the fabrication process flow for obtaining a stable a-C thin film on Si substrate with strong adhesion. Here, to develop the a-C film, we have used pyrolysis of negative photoresist material SU8, which also provides us with the added benefit of photo-patternability. One of the desired outcomes of the proposed work is to provide a reduced response and recovery time. Also, we have targeted to achieve a low limit of detection with high selectivity. Additionally, we have developed a readout circuit for chemiresistive sensors, where change in device resistance is used as a transduction principle for targeted analyte detection. The circuit is designed to meet the specification of the sensor, where the desired detection range extended up to a few hundred Mega ohms. The requirements of the system have been studied and implemented using Cadence. The prototype of the circuit has been designed and tested.

# Nomenclature

1. IoT : Internet of things
2. USB : Universal Serial Bus
3. LED : Light Emitting Diode
4. ADC : Analog to Digital Converter
5. CKT : Circuit

# Contents

# Chapter 1

# Introduction

Human activity is the biggest source of ammonia ($NH_3$) production. Ammonia is commonly used in industrial applications, including petrochemical, pulp and paper, fertilizer and the oil industry. Use of anhydrous $NH_3$ as a coolant in refrigeration systems as a replacement for environmentally unfriendly chlorofluorocarbon refrigerants is very common. Ammonia produced during industrial combustion is about 2.1-8.1 Tg/year [1]. The contribution of nitrogen fixation to the total worldwide $NH_3$ emission is approximated to be 1.0 Tg/year [2]. According to the European Environment Agency (EEA), almost 10 million metric tons of $NH_3$ are produced and used per year in Western Europe, making it one of the most common of all High Production Volume (HPV) industrial chemicals [3]. Liquid anhydrous ammonia (LAA) expands over 850 times when released to ambient air forming large vapor clouds normally lighter than air. LAA may also form an aerosol consisting in part of small liquid droplets of ammonia that are heavier than air and sink towards the ground leading to sudden drop in temperature and condensation of water vapour in the air forming a visible white cloud. Ammonia is a toxic gas that has given rise to serious environmental problems. The most widely recognized exposure limits of ammonia are of 25 ppm for a period of 8 h (time weighted average) and of 35 ppm for a period of 10 min (short term exposure limit) [3]. Ammonia is also corrosive to the skin, eyes, and lungs. Exposure to 300 ppm is immediately dangerous to life and health.

Given the toxicity of ammonia gas and its detrimental health effects, ammonia sensors are important devices in many industrial, agricultural and biomedical applications for continuous monitoring of the exposure level. There is also a strong need for reliable detection of $NH_3$ gas leaked into the atmosphere to control the environmental hazards and pollution caused by it. Ammonia is also used in human breath analysis as a biomarker to monitor, diagnose and detect renal diseases. Measurement of arterial ammonia has also been

used as a diagnostic test for hepatic encephalopathy [4]. Breath ammonia measurement may also be used as a diagnostic test for Helicobacter pylori infection [5]. Ammonia is used in heavy water plants as ammonia-hydrogen exchange process is a commercially viable heavy water production method. For example, owned and operated by the DAE's Heavy Water Board (HWB), the Talcher Heavy Water Plant in Odisha produces heavy water using the thermal version of the ammonia-hydrogen exchange process and has a production capacity of 72Mt of heavy water per year. Similarly, the Heavy Water Plant at Baroda is the first plant set up in India for the production of heavy water by employing monothermal Ammonia-Hydrogen exchange process. Hence ammonia detection schemes with potential applications in Breath ammonia measurement and heavy water plants can be of significant commercial and social importance.

Ammonia is the most important industrial raw material for many industries and one of the harmful gas to human beings and animals. Ammonia ranks second behind sulfuric acid in the quantity produced worldwide per year. Ammonia is used as a fertilizer, refrigerant in refrigerators water purifiers, explosives, textiles, pesticides and dyes. Ammonia is used in the manufacture of fertilizers such as ammonium sulfate, ammonium nitrate, ammonium hydrogen phosphate, and also used in Dyes, fibers and plastics and explosive such as ammonium nitrate, nitroglycerine and trinitrotoluene which is most commonly called as TNT. Ammonia is also naturally existing in human beings, animals and environment. It is a precursor for many biological processes, amino acids and nucleotide synthesis. In the environment, ammonia plays a major role in nitrogen cycle and it is produced in soil by bacterial process. Ammonia is also produced by decomposition of organic matter, including plants, animals and animal wastes.

At room temperature, ammonia is a colorless, highly irritating gas with pungent and suffocating odour. In pure form it is anhydrous ammonia and hygroscopic (means ammonia can absorb moisture). Ammonia gas easily dissolves in gas and forms ammonium hydroxide which is a weak base.

### 1.1.1 Immediate health effects of ammonia exposure

Ammonia is highly irritating and corrosive gas. On exposure of high concentration of ammonia will cause immediate burning of nose, throat and respiratory tract. When exposed to ammonia from inhalation of the gas or vapors. Since ammonia exists naturally and is also present in cleaning products, exposure may happen from many sources usually anhydrous ammonia is lighter than air generally it dissipates this can cause bronchiolar damage to the lungs and airway destruction results in respiratory distress or failure and inhalation of ammonia at lower concentrations will cause irritation in the nose throat and coughing. Ammonia gas is having a pungent smell which can give early warning but ammonia also cause olfactory fatigue or adaptation reduced awareness on one's long term exposure for lower concentrations.

Children are more prone to ammonia gas exposure as compared to adults because they are having greater lung surface area to body. Exposure of ammonia in air will cause rapid skin irritation and rapid eye irritation. High concentration of ammonia exposure will cause severe Injury and burns. Contact with concentrated ammonia solutions may cause corrosive injury including skin burns, permanent eye damage or blindness. Exposure to high concentration of ammonia by swallowing will cause severe damage to mouth and throat.

Usually ammonia interacts with the moisture in the skin, eyes, oral cavity and respiratory tract and cause damage to them in particular mucous surfaces will form anhydrous ammonia. Ammonium hydroxide will cause disruption of cell membranes which causes necrosis of tissues leading to the cellular destruction which is commonly called as saponification.

As the cell proteins are breaking down, water is extracted out from them which result in inflammatory response to cause further cell damage. We cannot treat ammonia poising by any antidote but we can people who is suffering from ammonia exposure and most of the people will recover from it. But to get completely recovered from ammonia exposure they should be treated with copious amounts of water to decontaminate eyes, skin is very important. Usually we can detect ammonia in blood and urine. But they are usually present in human body and animals. So they cannot be used as biomarkers of exposure.

### 1.1.2 Ecological effects of ammonia

Generally, most of the ammonia is produced by bacteria in the soil and in water as an end product of decomposition of animal bodies and plant bodies. Ammonia is in low concentration in soil, water and air. Ammonia in soil acts as a source of nitrogen in plants. Ammonia will go through many biochemical transformations in soil and water. All these collectively will form nitrogen cycle.

### 1.1.3 Ammonia in water

When ammonia reacts with water it forms ammonium and hydroxide ions. Ammonia is usually called as unionized ammonia. Ammonia is very toxic to aquatic animals but ammonium is nontoxic to aquatic animals. In most of the cases equilibrium exits between nontoxic ammonium and toxic ammonium.

The equilibrium between $NH_3$ and $NH_4$ + is affected by temperature and acidity (i.e. pH). Even a low concentration of ammonia 0.02 mg/L unionized ammonia is lethal to aquatic life.

### 1.1.4 Ammonia in air and soil

The vapors of ammonia will dissipate with the moisture in the air to form ammonium and eventually return to earth as rainfall. Ammonia will bind to the negatively charged soil organic matter and to the soil. Usually ammonium won't accumulate in the soil because bacteria will convert ammonium to the nitrates which can be easily absorbed by the roots of the plants.

If we suppress ammonia vapor cloud with the water, then it gets absorbed by the soil and can contaminate the soil. In such cases we need go for remediation to prevent further advert effects.

### 1.1.5 Ammonia affecting plants

Plants, trees and crops are made up of mostly water. If ammonia vapour is released into the atmosphere will likely burn the leaves of nearby vegetation. Ammonia will absorb water

from the leaves but it cannot damage the roots. So there is chance to recover out of it. But if may result in yield loss

### 1.1.6 Ammonia affecting livestock

Ammonia vapor in the atmosphere is toxic to the livestock.

## 1.2 Motivation for the project

There is a need to detect $NH_3$ in atmosphere and surroundings to save human beings, animals and plants. Traditional ammonia sensors can detect ammonia in the surroundings, but they operate at high temperatures (400 $^0$C- 600 $^0$C). This leads to high power consumption on the sensor, in addition to the need of developing a heating mechanism on the sensing platform. Fabrication of such heating elements are not easy, and are not cost effective. So there is need to detect ammonia at room temperatures, and at low cost.

The current thesis work focuses on design and fabrication of room temperature operated ammonia sensors, with reasonably good selectivity, sensitivity and responsivity.

## 1.3 Proposed Work

As reported in literature, most of the classical metal oxide gas sensors require to be operated at relatively high temperatures to achieve good sensitivity in ammonia detection. As opposed to this, here we propose to develop a room temperature gas sensor using an amorphous carbon – silicon heterojunction device. We aim to realize the amorphous carbon thin film using pyrolysis of negative photoresist material SU8, as a cost effective alternative to the conventional deposition protocols such as sputtering. Also, use of this polymer allows us to lithographically pattern the film, before pyrolysis, as per our requirement, which is itself a significant advantage. Further, as the polymer matrix can be reinforced with several materials like CNT, Graphene, metal oxides etc., the resultant carbon film can be made to have additional properties that may enhance its sensing behaviour. Here, we have used the heterojunction device to sense ammonia in low concentrations, using C~f characteristics (capacitance vs frequency), where change in the device junction capacitance upon exposure to the target gas is used as the sensing principle.

Additionally, we have targeted to develop read out circuits for chemiresistive sensor platforms. In general, chemiresistive devices are platform wherein change in the device's electrical resistance upon change in its surface conditions or environment is used as the transduction principle. For effective utilization of such platforms in point-of-care analysis, development of read-out circuitries and their integration with the sensor is essential. Keeping this in view, we have worked towards the development of such a read out circuit, where resistance of the target application ranges up to 100's of Mega ohms. The aim of this thesis can be summarized as follows:

- To fabricate amorphous-Carbon/Silicon based heterojunction for room temperature $NH_3$ sensing.
- To optimize the fabrication process flow for obtaining properly adhesive, stable a-Carbon thin film on Silicon substrate.
- Enhancement of the device sensitivity, and improving the limit of detection
- To develop a USB powered readout circuit, compatible with mobile, for chemiresistive sensor.

## 1.4 Thesis Organization

Chapter 2 discusses on literature survey on ammonia sensors working at different temperatures and with different sensitivities.

It is followed by Chapter 3, where the detailed fabrication process flow is explained along with different physical characterization and electrical characterization techniques used in this work.

Chapter 4 explains the working principle of the device and optimization of process flow. This chapter gives detailed explanation about material characterization with results and reports on sensitivity, stability and performance of the fabricated device.

Chapter 5 explains about the readout circuit design for chemiresistive sensor. It summarizes the results obtained with Cadence simulation. In chapter 6, the whole thesis is summarized along with the scope of further work.

# Chapter 2

# Literature Review

Several attempts have been made in the past to develop efficient sensors for ammonia. For instance, in [6], a quartz crystal microbalance transducer based ammonia sensor was proposed for monitoring the ammonia concentration in agricultural emissions. In this work, the authors have proposed a low cost sensor array for agricultural applications. The gas sensor array is fabricated on a quartz crystal microbalance transducer. They have optimized gas layers for selective detection of ammonia at varying humidity conditions. In this paper, the authors have studied different porous material properties and their performance towards ammonia detection.

Moos et al. [7] developed another ammonia gas sensor with a selective thick film of zeolites for automotive exhaust gas applications. Using ammonia, they were able to reduce $NO_X$ emissions in the automotive exhaust. In this work, ammonia gas sensor is employed to detect the presence of ammonia in the exhaust. The authors have found Zeolite as the functional material for such kind of sensor in this range of applications. They have optimized working temperature and working frequency to determine selectivity and sensitivity of the sensor.

Pushkarsky et al. [8] presented a laser-based photo-acoustic ammonia sensor for industrial ammonia gas measurement. In this work, they presented resonant cavity based techniques to detect gases. They have proposed an idea to measure intra-cavity electromagnetic field behavior which change the cavity properties and medium loses through which one can detect gases.

Zakrzewska et al. [9] developed metal oxide ammonia sensors using tin oxide as the sensing material. In their paper, the authors have carrier out their work on mixed oxides such as $SnO_2$-$WO_3$, $TiO_3$-$WO_2$ and $SiO_2$-$TiO_2$. They have prepared materials in the form of polycrystalline ceramics and thin films by a variety of methods which include impregnation, co-precipitation and sputtering. Simple metal oxides such as $SnO_2$, $WO_2$, and $TiO_2$ are commonly known for the high sensitivity to change in surrounding gases in the environment.

Usually commercial gas sensors for hydrogen, methane and carbon dioxide presence can be detected using $SnO_2$. They operate at a temperature of 300 $^0$C to 400 $^0$C. They are called as surface sensors because the interaction between and gas molecules will happen according to the adsorption principle. One of the other class of material that can detect is Titanium dioxide in which bulk diffusion determines the sensor responsivity. These sensors operate at a temperature range of 1000 $^0$C to 1200 $^0$C.

## 2.1 Mixed metal oxides as ammonia sensing material

Mixed oxides are promising materials for gas sensing applications. They can give improved sensing properties compared to normal oxides. Several mixed metal oxides, such as ZnO-$SnO_2$ compounds ($ZnSnO_3$ and $Zn_2SnO_3$), $TiO_2$-$SiO_2$ compounds have been used in the past for such applications. These metal oxides are formed by the modification of electronic structure of the system. It has been concluded that equilibration of the Fermi level throughout the mixed oxide semiconductor is responsible for its electrical and gas sensing properties. It has also been verified that $SnO_2$-$TiO_2$ has a great potential as a gas sensing material.

Using a $WO_3$ ammonia sensor with Au and $MoO_3$ additives, researchers developed a semiconductor sensor to detect residual ammonia in the combustion exhaust [10]. In this work the authors found that WO3 is sensitive to both $NH_3$ and NO. They decreased the sensitivity to NO by mixing $MoO_3$ by weight percentage. They fabricated ammonia sensor with Au (0.8 wt. %) – $MoO_3$ (5 wt. %) – $WO_3$ which can sense ammonia in the range 1-50 ppm. The operating temperatures for these sensor was found to be in range of 400 $^0$C to 500 $^0$C. $MoO_3$-Au-$WO_3$ is found to have quick response time and high sensitivity to ammonia without disturbing the effect of NO. They have followed three methods, painting,

impregnation and evaporation respectively. Finally, the authors have fabricated a semiconductor sensor by modifying $WO_3$ based elements with $MoO_3$.

In another work [11], researchers developed a surface acoustic wave gas sensor for monitoring low concentration ammonia. In [12], a chemical surface acoustic wave based sensor array for detection of Ammonia gas was reported.

## 2.2 Polyaniline as ammonia sensing material

Huang et al. [13] developed polyaniline nanofibers using interfacial polymerization at an aqueous and organic interface, and the resulting polyaniline, which had high surface area and porosity, could enhance properties in applications such as chemical sensors. With the same synthetic method, Virji et al. [14] fabricated polyaniline nanofiber gas sensors with performances that were better than conventional polyaniline.

## 2.3 Ammonia sensors using Micro electromechanical systems (MEMS) technology

Microelectromechanical systems (MEMS) technology was applied to fabricate various micro sensors. The advantages of micro sensors include small size, high performance, low cost and easy mass-production. Many studies have recently utilized MEMS technology to manufacture ammonia sensors.

For instance, fabrication of a CMOS- MEMS based ammonia gas sensor using polyaniline nanofibers along with integrated electronics was reported in [15]. The fabrication of the ammonia sensor included a post- process etching of the sacrificial layers to expose the sensing resistor, and then the ammonia sensing polyaniline film is coated on the sensing resistor. The ammonia sensor was based on the resistive change of the sensing film upon adsorption or desorption of ammonia gas. A readout circuit was employed to convert the resistance of the ammonia sensor into the voltage output. Experimental results showed that the sensitivity of the ammonia sensor is about 0.88 mV/ppm at room temperature.

Mitzner [16] reported a micro-hotplate- based gas sensor array for detection of ammonia, methane and hydrogen sulfide. The post-CMOS process adopted $XEF_2$ to etch a silicon

substrate to obtain the micro-hotplate-array, and $SNO_2$/Pt sensing film was sputtered on this micro-hotplate forming a resistive-type ammonia sensor. The principle used therein is the change in resistance when a metal oxide is exposed to gas, depending on the type of the gas used. Usually gases like $CH_4$, $H_2S$, $NH_3$ act as reducing agents, and add electrons to the metal oxide material, which result in increase in electron concentration thereby increasing the conductivity. Metal oxide sensing films doped with noble metals are reported to have good sensitivity and decreased response time.

Figure 2-1 shows the resistance change in the $SnO_2$/Pt film fabricated in this paper. The film was exposed twice to 1000 ppm $NH_3$ at 200 sccm. The initial baseline of the resistance was found to be 126 kΩ whereas after $NH_3$ exposure base line came to 500 kΩ. In this work there is a shift in base line after exposure but the magnitude of the baseline shift decreased with successive exposures. This shows after the exposure of the gas there is significant change in baseline. This shows that this sensor cannot be effectively used as $NH_3$ sensor.

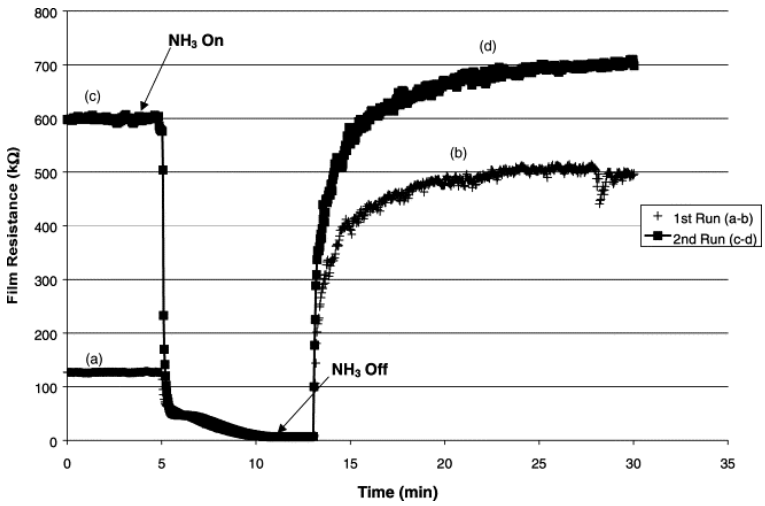


**Figure 2-1 Exposure of SnO2 film to NH3 and baseline shift**

The relative normalized gas responses for different gas exposures on $SnO_2$/Pt films are shown in the below figure. The data in Figure 2-1 show that $SnO_2$/Pt film is more sensitive to ammonia compared to other gas exposure.

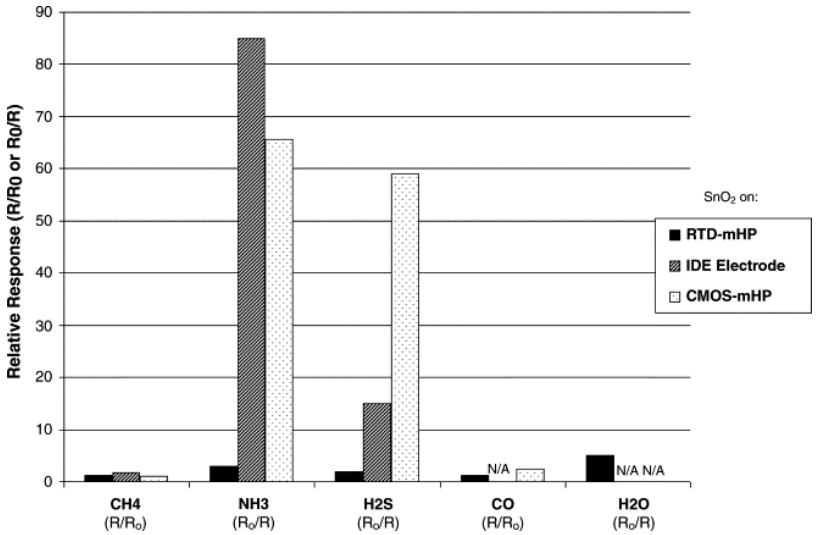


**Figure 2-2 Selectivity analysis of SnO2/Pt film to different gases**

Lobet et al. [17] utilized silicon process technology to make an ammonia sensor, in which the sensor consisted of a heater, an interdigital electrode, a temperature meter and a sensing film. Tungsten oxide, coated on the interdigital electrode, was adopted as an ammonia sensing film. Li et al. [18] presented a micro gas with piezo resistive $SiO_2$ cantilever beam fabricated by a surface and bulk micromachining process. An ammonia sensing layer of 11-mercaaptoundecanoic acid was coated on the piezo resistive cantilever beam.

## 3.1 Thin film metal oxides as ammonia sensing material

Prasad et al. [19] reported ammonia sensing characteristics of thin film based on polyelectrolyte template polyaniline. In this work they have synthesized polyaniline using poly (4-styrenesulfonate-co-maleic acid) as counter ion and template. The resistance of this polymer increases when exposed to gases like ammonia. When spun cast on glass substrate, the film was able to detect gases in the concentration of 5-250 ppm. The resistance response time was found to be 150s. Usually, conducting conjugated films offers a lot of advantages because of the ease in chemical synthesis and thin film fabrication techniques

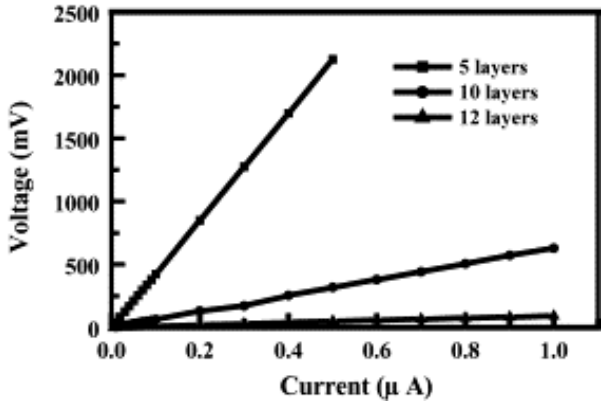


**Figure 2-3 I-V characteristics of PANI thin films with different layers**

The authors have fabricated a water soluble polyelectrolyte (PSSM) template PANi film. The ammonia sensing capabilities of the film were observed. They found 5 layered film as the most suitable one for ammonia detection. Characteristics of PANI thin film is shown in Figure 2-3.

Sadanand Pandey and coworkers [20] reported a silver nano particle based flexible ultrasensitive nanocomposite resistive sensor for ammonia detection. The reported nanocomposite can detect ammonia as low as 500 parts-per-trillion at room temperature in a minute's time. Mariappan et al. [21] reported about ammonia sensing with Na doped zinc oxide thin film nanorods prepared using nebulizer spray pyrolysis technique. Gopal Goswami [22] reported detection of aqueous ammonia using surface plasmon reaction with polysaccharide gold nano particle composite. Response time of 10 sec and detection limit of 1 part per billion was reported in the same study. C N R Rao et al. [23] reported ammonia sensors based on catalytic oxides such as $V_{2O5}$, $MoO_3$ and α, β- and γ-bismuth molybdates. $MoO_3$ (15 mo1%) supported on $TiO_2$ and γ-$Bi_2MoO_6$ both was reported to exhibit satisfactory sensing characteristics for $NH_3$, with a reasonably low working temperature (500-575 K) and a minimum detection limit of 10 ppm. C N R Rao et at. [24] also reported ammonia sensors based on metal oxide nanostructures. Somnath Roy [25] reported a novel ammonia sensing phenomena in sol-gel derived $Ba_{0.5}Sr_{0.5}TiO_3$ thin films. Somnath Roy et al. [26] also reported about the enhancement of ammonia sensitivity in swift heavy ion irradiated nanocrystalline $SnO_2$ thin films. Xue et al. [27] reported Ammonia sensors based on a-C/Si heterojunction using SU 8 as a precursor material by sputtering.

# Chapter 3

# Device Fabrication Process flow, Electrical Characterization and Physical Characterization

## 4.1 Fabrication Process

A generalized fabrication process flow was followed in the fabrication process which includes cleaning of the wafer, spin coating of the photoresist on the wafer, pattering the device, photoresist removal and optimization of temperature profile for the pyrolysis process followed by development of electrodes.

### 4.1.1 Chemical Compounds used for fabrication

SU-8 2005 (Microchem, USA) Photoresist, SU-8 Photoresist developer, Sulfuric acid ($H_2SO_4$), Hydrogen Peroxide ($H_2O_2$), De-Ionized water, Ammonium Hydroxide ($NH_4OH$), Titanium target, Buffered oxide.

### 4.1.2 Equipment and glassware required

Optical lithography (SUSS MicroTec, Germany), DC Sputtering (AJA Internationals, USA), Glass beakers, Micropipette, Glass flask, Inert chamber furnace

## 4.2 Device Fabrication Process Flow

Fabrication process of the device was carried out in a class 10000 clean room environment. The process flow involves multiple steps. Process parameters associated with each step have been optimized properly to achieve optimal results. The a-C thin film was formed on n-type silicon substrate. Steps in the fabrication process are presented in the flowchart in and explained in detail in subsequent section.

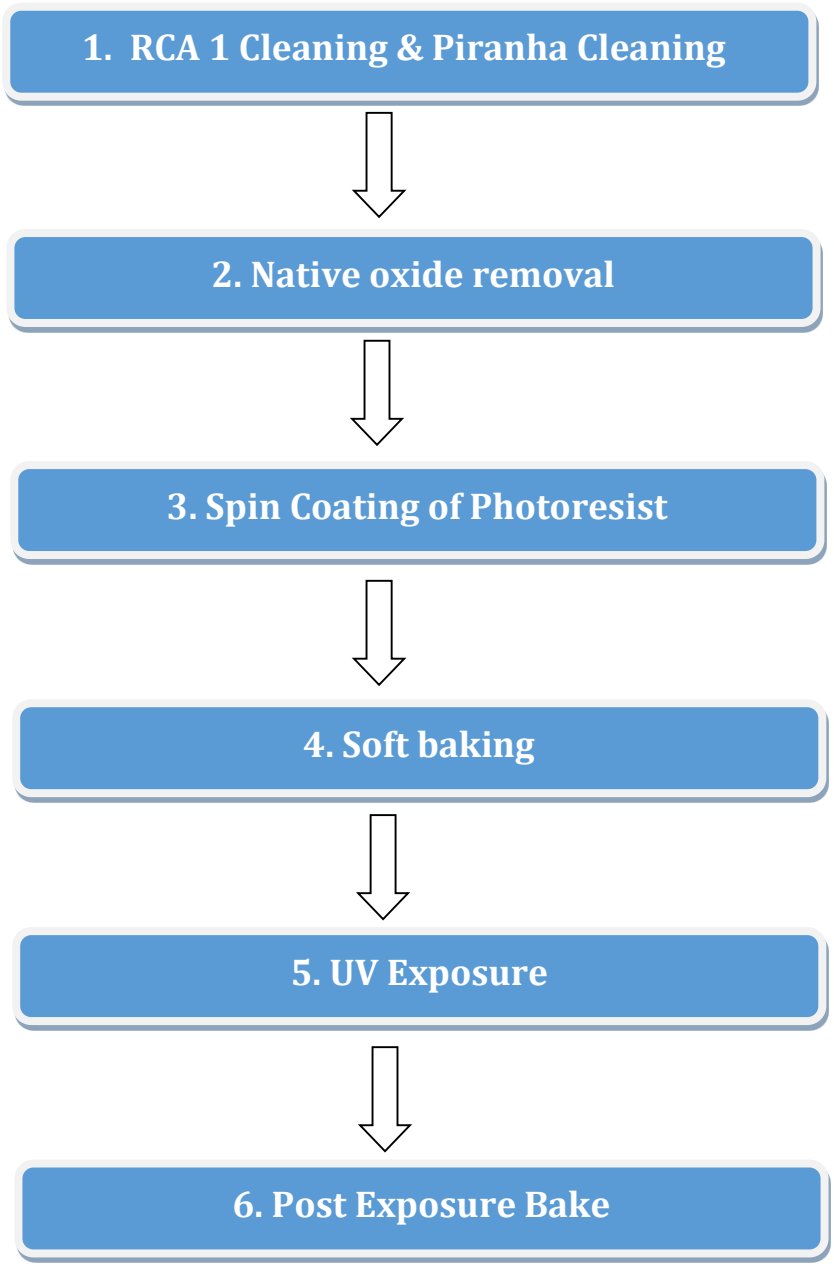

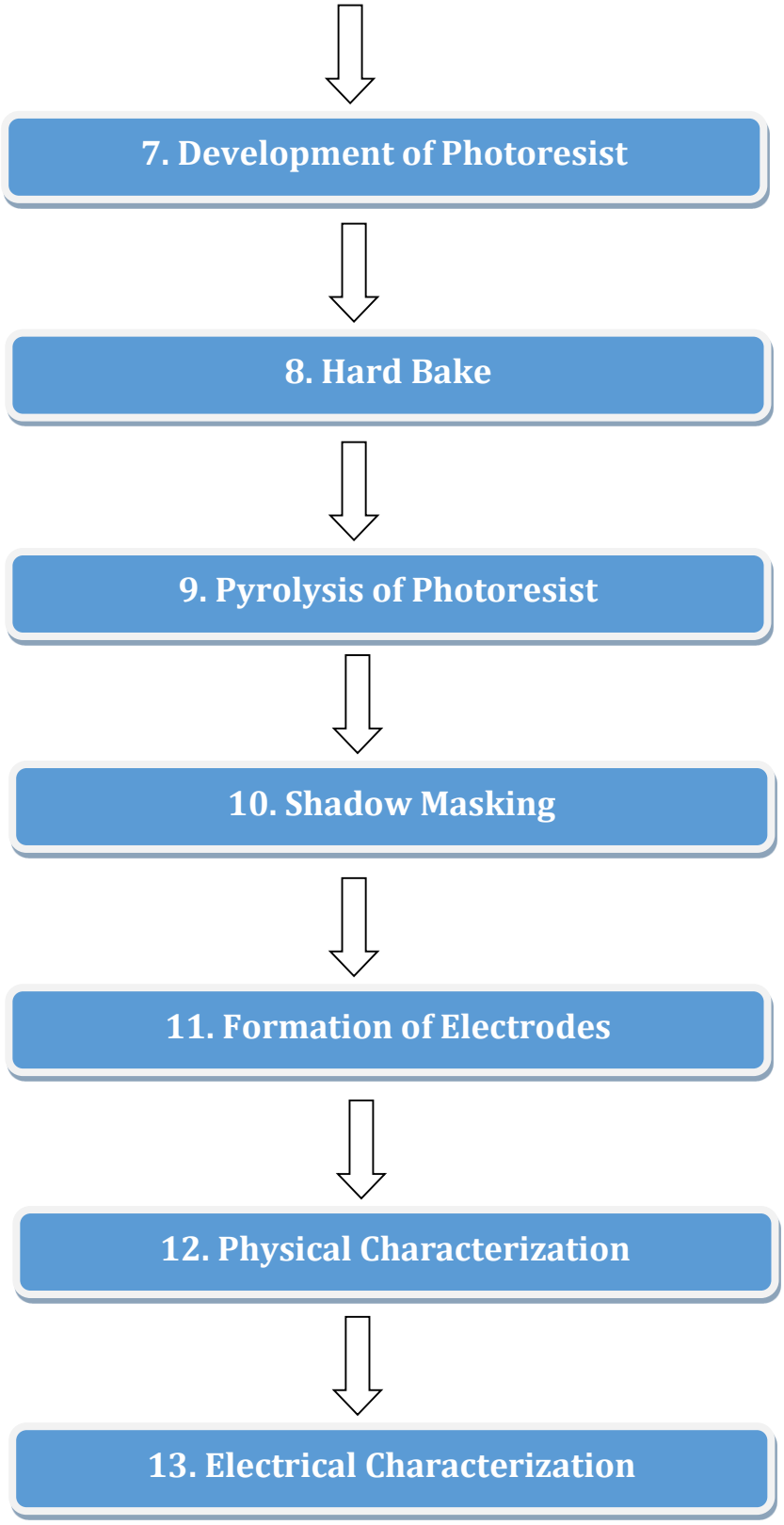
7. Development of Photoresist
8. Hard Bake
9. Pyrolysis of Photoresist
10. Shadow Masking
11. Formation of Electrodes
12. Physical Characterization
13. Electrical Characterization

### 4.2.1 Wafer Specification

For the fabrication of the device a four inch, n-type (phosphorous doped) prime grade wafer with <100> orientation was selected.

### 4.2.2 RCA 1 Cleaning and Piranha Cleaning

RCA 1 is a mixture of Hydrogen Peroxide ($H_2O_2$) and Ammonium Hydroxide ($NH_4OH$) in the ratio of 5:1. Piranha is mixture of concentrated sulfuric acid ($H_2SO_4$) and Hydrogen Peroxide ($H_20_2$) in the ratio of 3:1. RCA 1 Cleaning and Piranha Cleaning is necessary step to remove any metallic and organic residues from the wafer.

### 4.2.3 Lithography

Lithography is one of the important process in micro fabrication. It is used to pattern the photoresist which is deposited on the wafer. Two kinds of photolithographic techniques are used in this thesis work. Laser writer was used to prepare masks and Photolithography was used to pattern SU-8 photoresist. In this step , UV lamp which is having a wavelength of 293 nm is used as the source.

Photoresist is the sacrificial layer deposited on the substrate to enable patterning. There are two kinds of photoresists 1. Positive Photoresist 2. Negative Photoresist. For a positive photoresist the polymer chains will break on exposure to UV light and exposed area becomes soft and can be removed by using a developer. For a negative photoresist the polymer chains will get cross linked on exposure to UV light and becomes hard the remained unexposed area can be removed by using a developer. In this work, SU-8 (negative photoresist) and SU-8 photoresist developer was used in the fabrication process flow.

### 4.2.4 Selection of Photoresist material

Photoresists are commonly used as masking materials for photo-lithographic pattern, but they can also be used as structural materials instead of being stripped away. Many types of photoresists are used in the MEMS fabrication techniques. Among them, SU-8 Photoresist has its own significance. SU-8 is extensively used to form large aspect ratio thick structures. Polyimide, which is a major ingredient in photoresist, occurs in two forms: photosensitive form and non-photosensitive form. Non-photo sensitive polyimide is used in printed circuit boards. Photosensitive polyimide is used in photoresists.

Usually pyrolysis of the photoresist material in an oxygen free atmosphere leads to the formation of carbon leaving behind volatile materials. Positive photo resists based on novolak/diazonaphthoquinone resins, consist of predominantly aromatic polymers that are extensively cross-linked and are rendered soluble by exposure to ultraviolet (UV) light. While negative photo resists consist of rubber like polymer material that is predominantly aliphatic and a photosensitive cross-linking agent that cross links the polymer upon exposure to UV light. Because of its ability to convert into carbon after pyrolysis procedure we use SU-8 photoresist in the fabrication process.

The process with following steps was carried out to fabricate the amorphous carbon/Silicon hetero-junction device.

1. Initially a four-inch n-type (phosphorous doped) silicon wafer with <100> orientation is treated RCA 1 cleaning in which a solution of Hydrogen peroxide ($H_2O_2$) and Ammonium Hydroxide ($NH_4OH$) was taken in ratio of 5:1 and its temperature was raised up to 90 $^0$C, following which the wafer was dipped in that solution for 30 min.
2. In the second step the wafer is treated with piranha solution. In this step, the wafer was dipped for 5 min in a mixture of Sulphuric acid ($H_2SO_4$) and Hydrogen Peroxide ($H_2O_2$) in the ratio of 3:1, where the solution temperature is raised up to 90 $^0$c and.
3. Then the wafer was dried with compressed air.

4. The silicon wafer was treated with buffered oxide to remove any traces of native oxide formed on the substrate.
5. 1 ml of SU-8 photoresist was spread on the Si substrate and subsequently spin-coated at an rpm of 500 for 5-10 seconds with acceleration of 100 rpm/second. The subsequent step of the spin-coating was performed at 4000 rpm for 30 seconds with acceleration of 500 rpm/second.
6. Then the device was subjected to soft baking at a temperature of 120 $^0$C for about 2 minutes to evaporate the solvent.
7. The substrate was patterned with optical lithography (SUSS Micro Tec, Germany) using flood exposure mode for 30 seconds with the illumination of UV lamp of 396 nm wavelength.
8. Post exposure bake was done at 95 $^0$C for 3 minutes
9. The patterns formed on the photoresist were developed by using SU-8 developer by dispersing the substrate in the developer for 1 minute and shaking the beaker continuously.
10. Then, the samples were inserted in the furnace for pyrolysis. An inert ambient was created in the chamber by releasing 1.5 bar commercial nitrogen in to it. The following temperature profile (Figure 4-1) was followed in the furnace to generate carbonized thin film on the top of substrate.

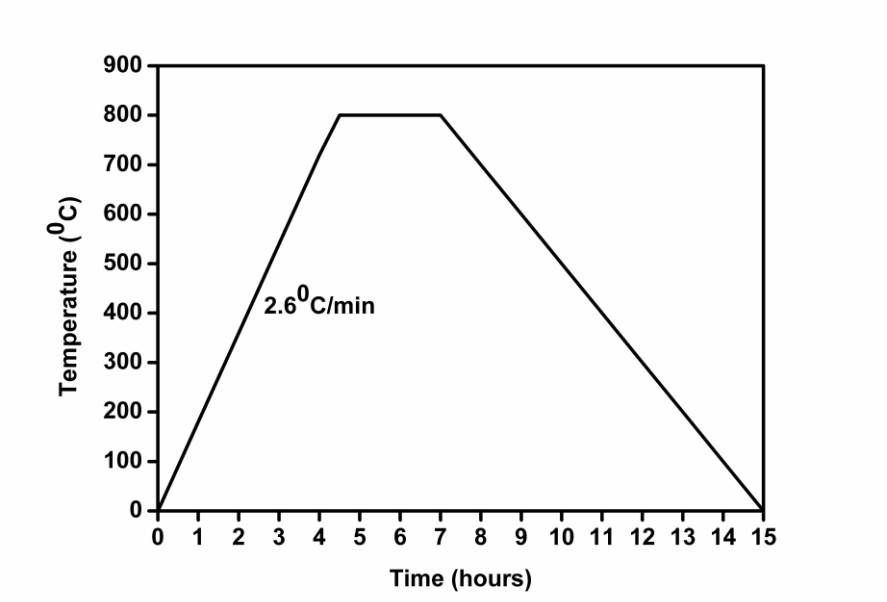


**Figure 4-1: Temperature Profile of the furnace**

11. The device was then removed from the furnace and a shadow masking technique was used to form 2mm*2mm titanium electrodes using sputtering.
12. Subsequently, physical characterization and electrical characterization of the device were carried out.

The diagrammatic representation of the device after each step can be seen in the Figure 4-2 shown below and device structure is shown in Figure 4-3

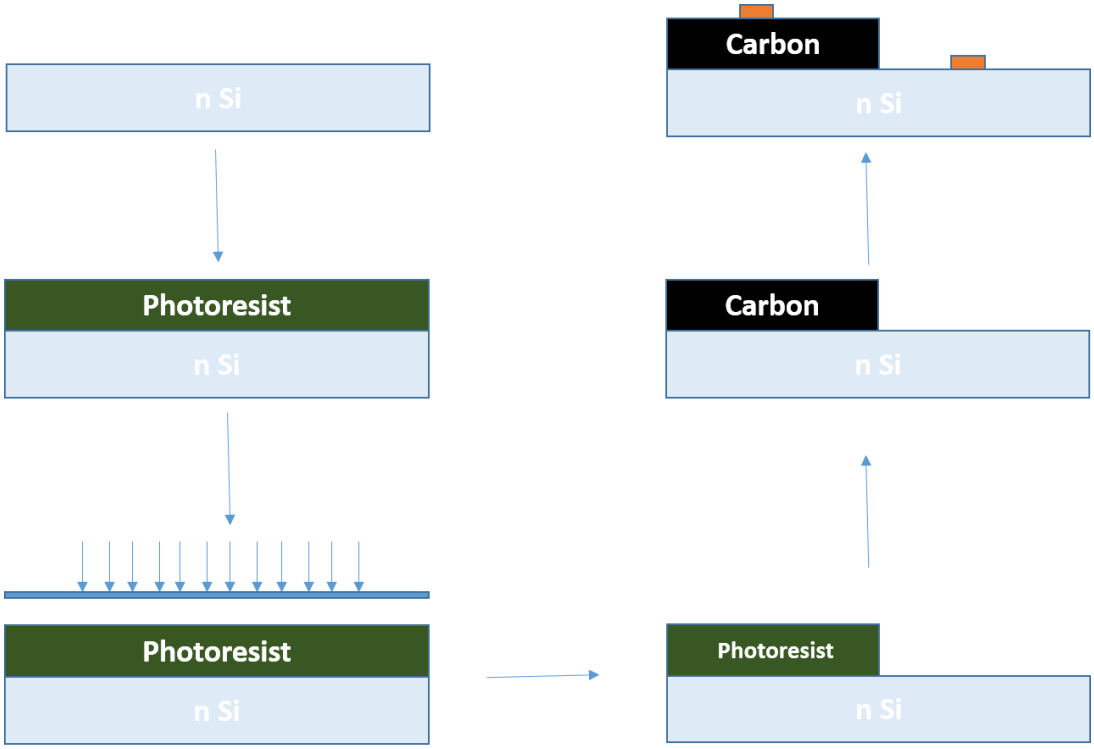


**Figure 4-2 Diagrammatic representation of device after each step**

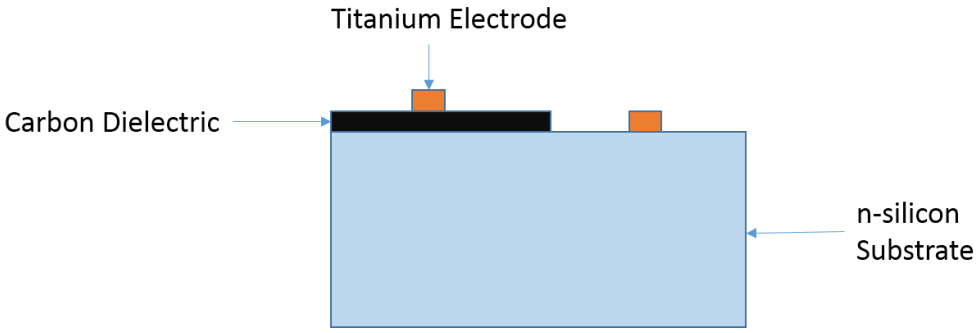


**Figure 4-3 Fabricated device with electrode**

## 4.3 Material Characterization

After the fabrication of the device by the procedure given in the above description following material characterization techniques were used.

- Scanning Electron Microscopy ( SEM )

  SEM was used to study the morphology of the film, the development of patterns on the film and the electrode-thin film interface.

- AFM

  AFM was performed on the sample to study surface roughness of the samples prepared at different pyrolysis temperature.

- Raman Spectroscopy

  Raman spectroscopy was performed on the samples prepared at different temperatures to study whether the formed thin films are crystalline or amorphous.

## 4.4 Electrical Characterization

To measure the capacitance of the amorphous Carbon/ Silicon heterojunction, Agilent semiconductor parametric analyzer (B1500A) along with a Cascade probe station was used. Schematic setup for the electrical characterization is as shown in
Figure 4-4.

The C~f analysis was carried out in the range of 1 KHz-1 MHz, with the peak capacitance being observed at 1 KHz at a contact potential of 0.2V.

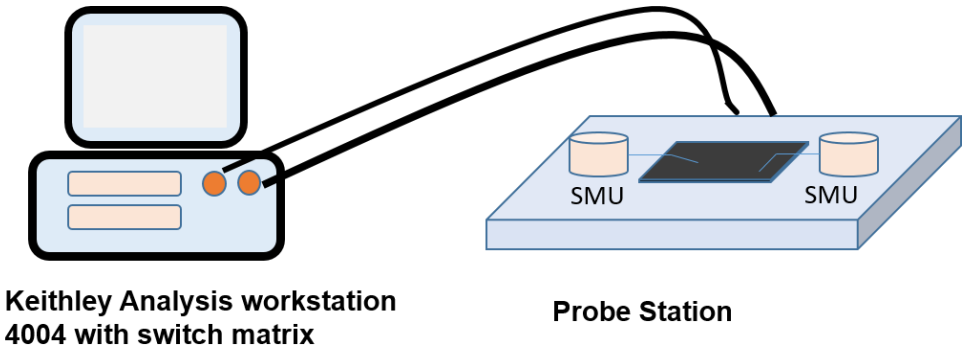


**Figure 4-4 Schematic for electrical characterization**

# Chapter 4

# Results and Discussion

## 5.1 Working Principle of the device

The change in capacitance of a-C/Si hetero-junction can be explained by adsorption process. Upon exposure of a-C film to $NH_3$, the $NH_3$ molecules gets adsorbed on the carbon film which results in change in contact barrier potential. The barrier potential of a-C/Si hetero-junction can be explained by the equation

$$C_T = A\sqrt{\frac{\varepsilon_1 \varepsilon_2 e N_D N_A}{2(N_D + N_A)(V_D - V)}}$$

Where e=1.602*$10^{-19}$, A is the a-C/Si hetero-junction interface area, $N_A$= hole density in the a-Carbon film $N_D$ is the electron density of the silicon , $V_D$ is the barrier potential and V is the applied voltage.

$NH_3$ molecules have the capability to donate electrons to carbon materials due to adsorption process [27]. On exposure of a-C/Si hetero-junction to $NH_3$ molecules, $NH_3$ molecules get adsorbed to the carbon film by replacing pre adsorbed molecules due to different adsorption energies of the molecules. As electrons are transferred from $NH_3$ molecules to carbon film, the Fermi level of the a-Carbon film will increase resulting in decrement of difference between Fermi levels of a-Carbon and n-Silicon which results in change in barrier potential.

As a result of the whole process barrier potential will decrease after adsorption of $NH_3$ molecules increasing capacitance after adsorption. After that when exposed to air, $NH_3$ molecules gets desorbed from the surface of the a-Carbon resulting in change in Fermi level due to release of electrons from a-Carbon film to $NH_3$ molecules.

## 5.2 Experimental Results

### 5.2.1 Material Characterization

SEM images of the fabricated devices are taken in order to make sure that pattern transferred on the film is having same finger width or not. Figure 5-1 shows unpatterned device and Figure 5-2 shows Titanium electrode on the a-Carbon film. Figure 5-3 shows patterned device with fingers. Figure 5-4 shows SU-8 patterned device which is having fingers of width 100 um and spacing between two fingers is 100 um.

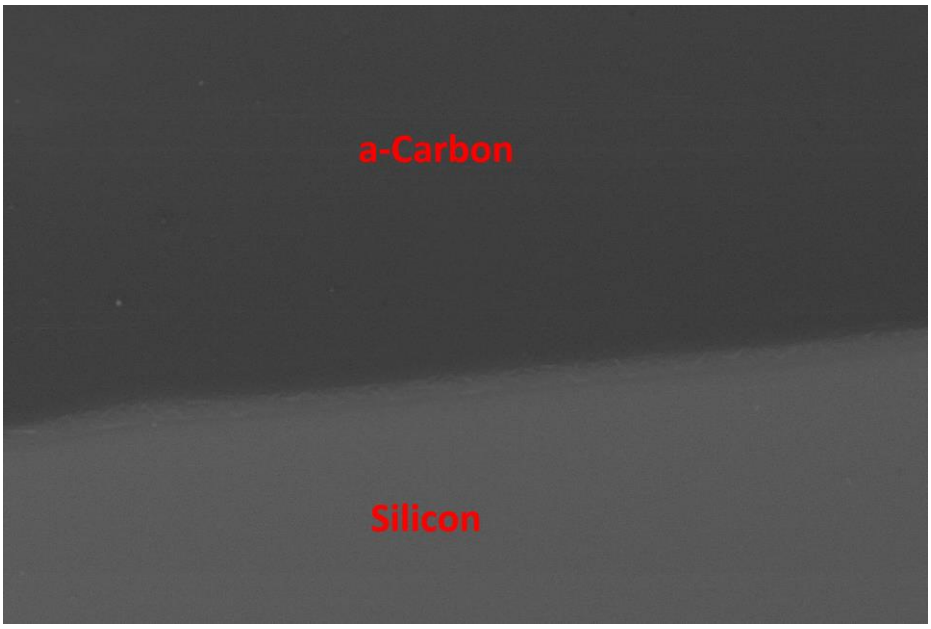


**Figure 5-1 SEM image of unpatterned device**

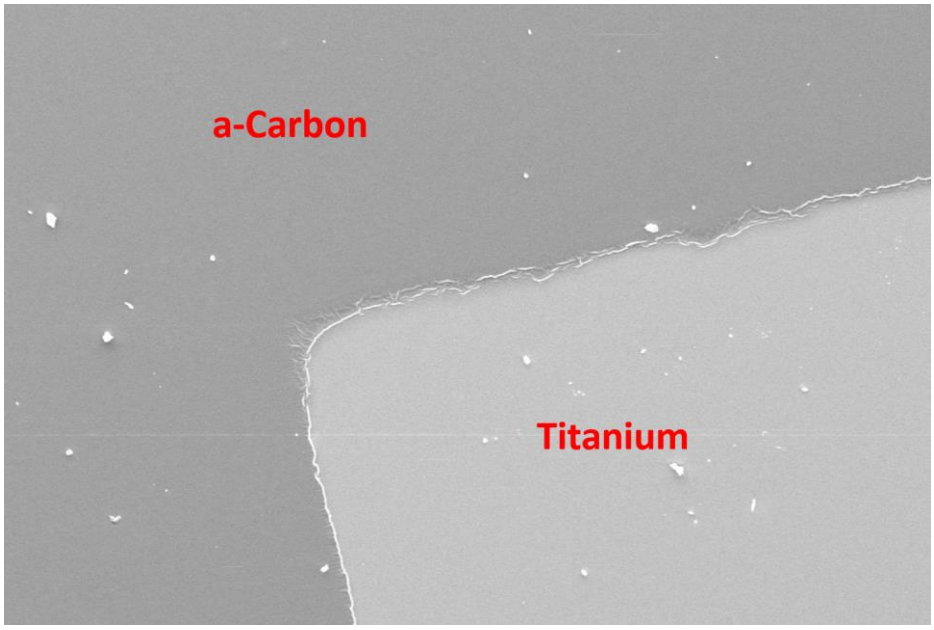


**Figure 5-2 SEM image showing Titanium electrode of 200nm thickness**

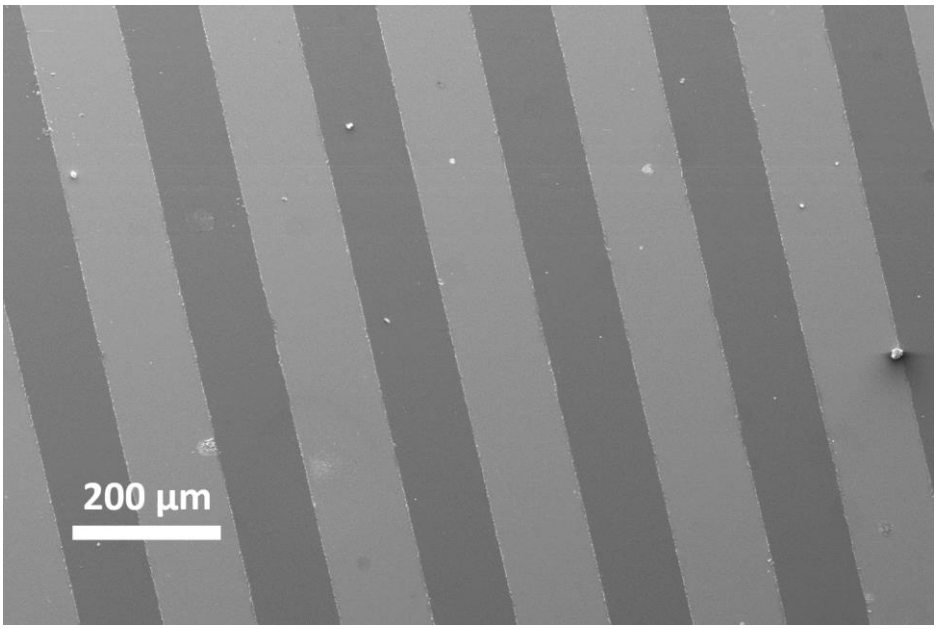


**Figure 5-3 SEM image showing finger pattern on the device**

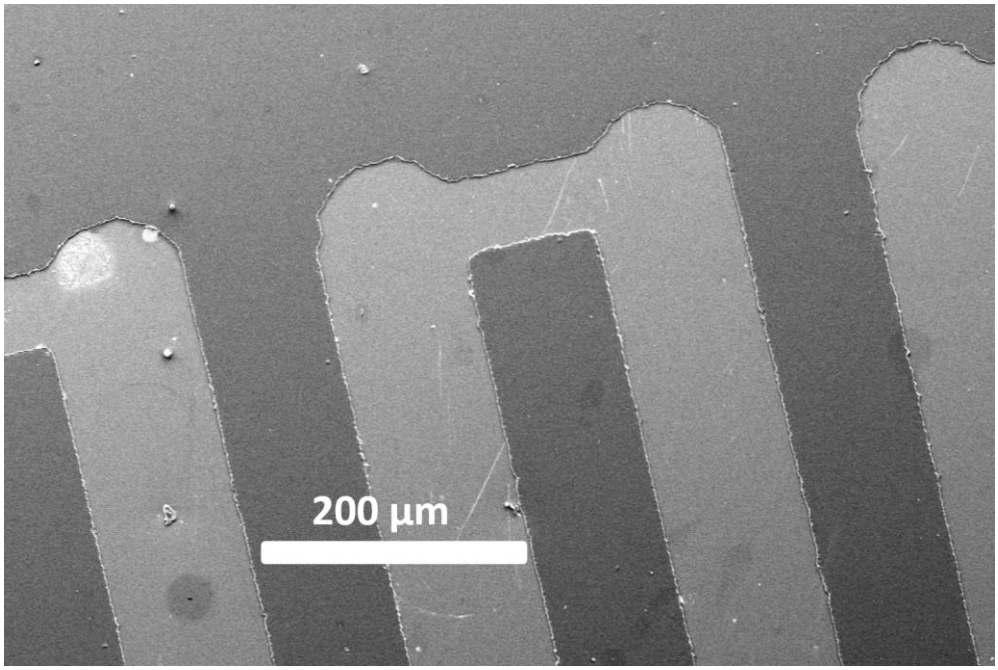


**Figure 5-4 SEM image of patterned device**

Raman spectroscopy is a nondestructive method which is used characterize diamond like carbon or polymer like carbon thin films. Figure 5-5, Figure 5-6, Figure 5-7 shows the Raman spectroscopic results of the carbon films at different temperatures and from the image, it can be inferred that the height of the D and G peaks are similar indicating the presence of a mixture of $sp^2$ and $sp^3$ hybridized states with no long-term crystallization [5]. The conclusion drawn forth can be that the film attains an amorphous nature at the process temperature.

The ID/IG ratio of the Raman Spectroscopy graphite crystallize size $R_a$ is inversely proportional to the

$$\frac{I_D}{I_G} \infty \frac{1}{R_a}$$

Effect of the pyrolysis temperature on the a-C film is tabulated in Table 1.

| Sl.No | Device description | Pyrolysis Temperature | $I_D/I_G$ Ratio |
|---|---|---|---|
| 1 | SU-8 2005 ( 5 µm) | 800 $^0$C | 0.85 |
| 2 | SU-8 2005 ( 5 µm) | 750 $^0$C | 0.83 |
| 3 | SU-8 2005 ( 5 µm) | 700 $^0$C | 0.81 |

**Table 1 Effect of Pyrolysis Temperature on Carbon film**

It has been observed that with pyrolysis at 700 $^0$C, we were able to get a carbonized film which is amorphous. With increase in the pyrolysis temperature, the amount of crystallinity in the film increases, which is indicated by the decreasing $I_D/I_G$ Ratio, where $I_D$ and $I_G$ stand for the D and G peaks respectively.

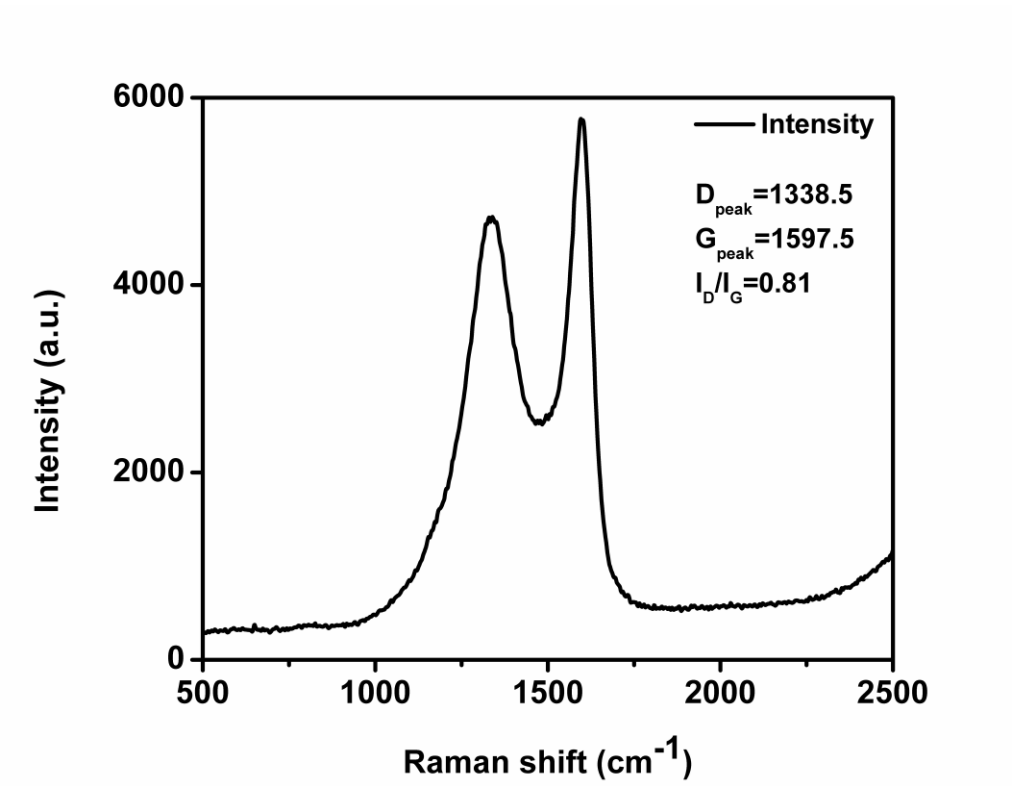


**Figure 5-5 Raman Spectroscopy of thin film at a temperature of 800 $^0$C**

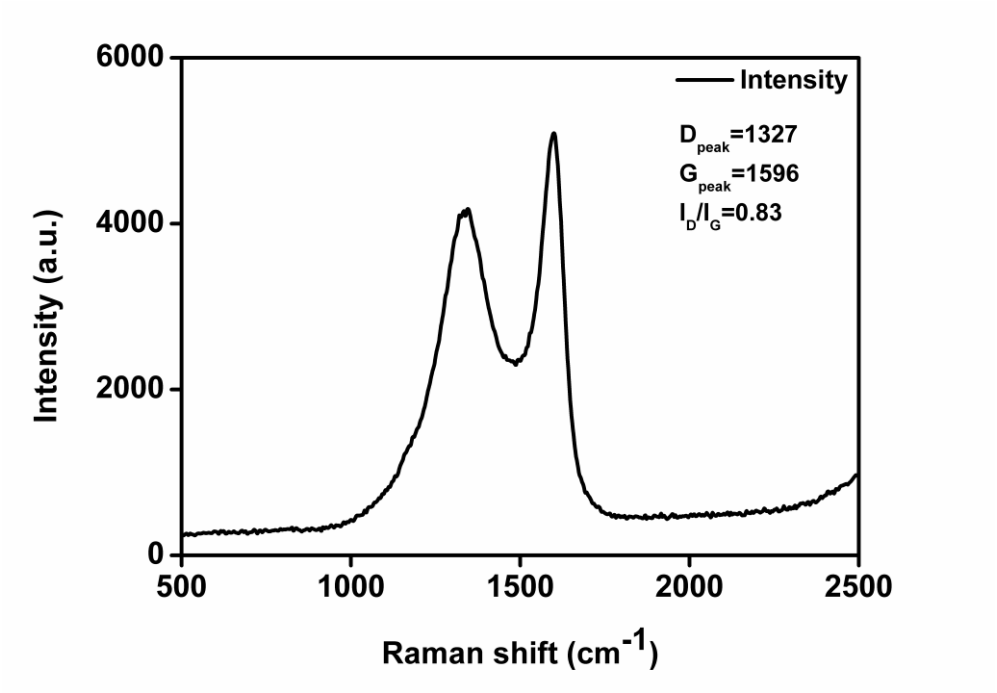


**Figure 5-6 Raman Spectroscopy of thin film at a temperature of 750 $^0$C**

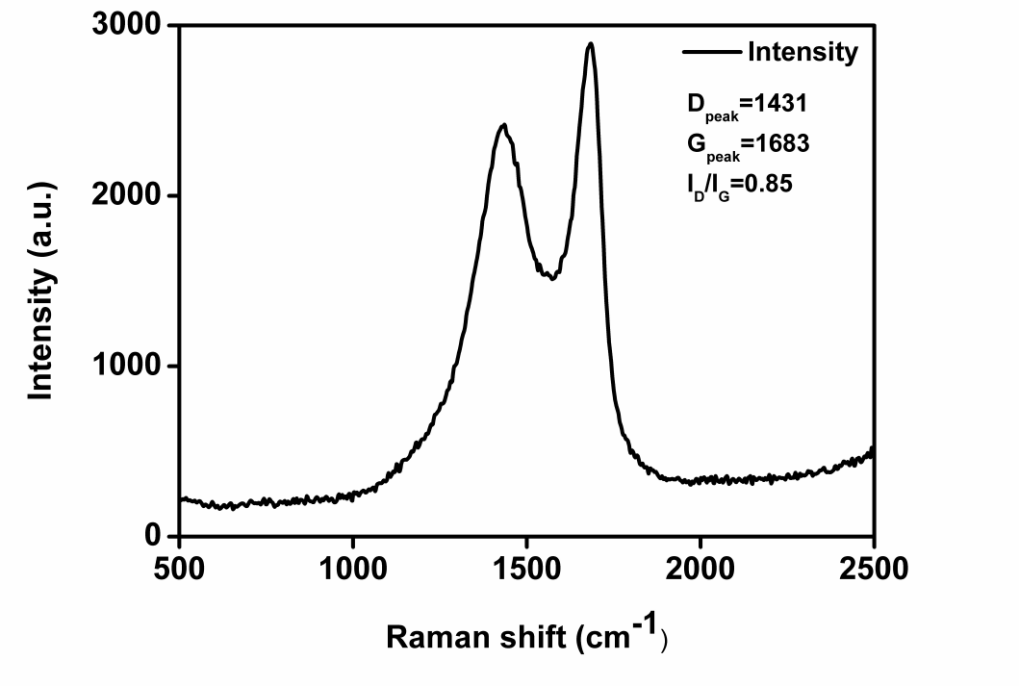


**Figure 5-7 Raman Spectroscopy of thin film at a temperature of 700 $^0$C**

In addition to the amorphous nature, film adhesion is another major challenge in fabrication process which has been addressed by carefully maintaining the proper temperature ramp profile during pyrolysis and hard baking. We have also performed Ellipsometry to analyse the relative permittivity of the carbon film, which can be approximated to 2.9.

Atomic Force Microscopy (AFM) results, shown in Figure 5-8, display the mean squared roughness and the average roughness to be in the range of 0.5 nm to 1.5 nm respectively. Surface roughness of the a-C film plays an important role in determining the $NH_3$ adsorption efficiency.

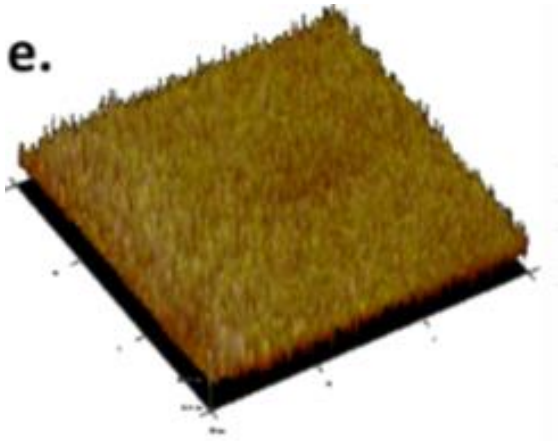


**Figure 5-8 AFM image of a-Carbon thin film show surface roughness**

## 5.3 Electrical Characterization

Ammonia is exposed to the a-Carbon/Silicon hetero-junction by heating ammonium hydroxide ($NH_4OH$) at a temperature of 70 $^0$C which results in dissociation of ammonium hydroxide ($NH_4OH$) into ammonia and water vapor.

The results presented in Figure 5-9 shows the response and recovery events of an unpatterned a-C film based device after exposure of $NH_3$. It can be inferred from the figure, the device shows an appreciable value of $\Delta C$ upon exposure to $NH_3$, indicating excellent responsivity to $NH_3$ exposure.

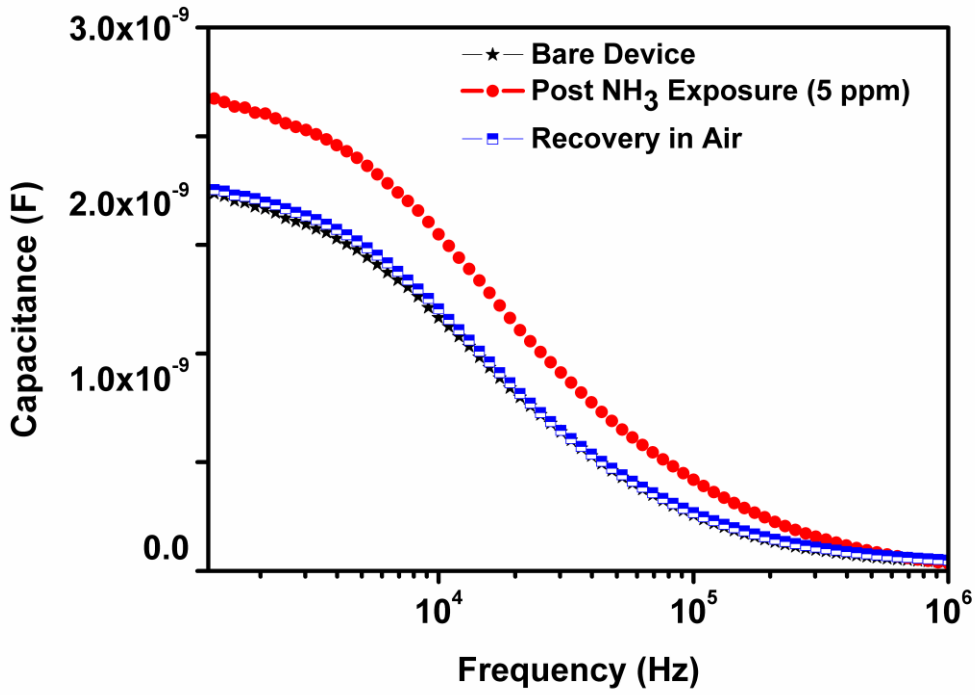


**Figure 5-9 C~f curves showing response and recovery events of an unpatterned a-C film based device**

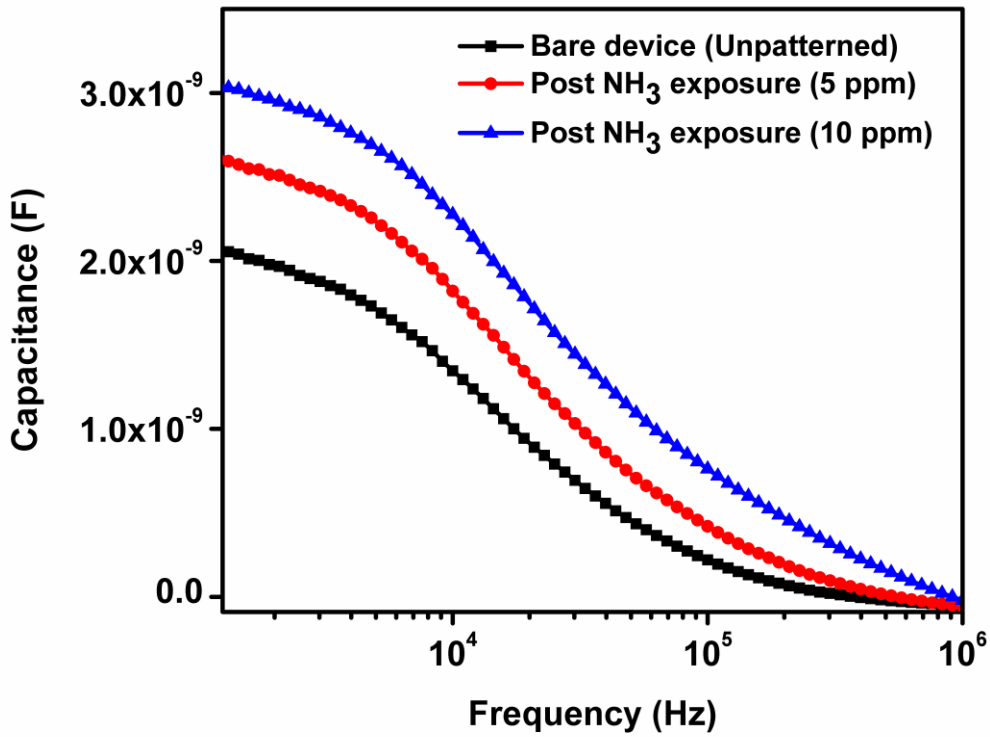


**Figure 5-10 C-f characteristics of a-Silicon/Carbon hetero-junction for different concentrations of NH3 exposure**

C-f characteristics for different concentrations of $NH_3$ exposure are shown in Figure 5-10. With increase in the target dose, the junction capacitance increases significantly. For an exposure dose of 5 ppm, a change of 27% $\Delta C$ was recorded. For an exposure dose of 10 ppm, a change of 48 % was recorded. With increase in the gas concentration, the amount of $NH_3$ adsorbed on to the device also increases, increasing the excess charge carriers, which proportionally decreases the barrier potential.

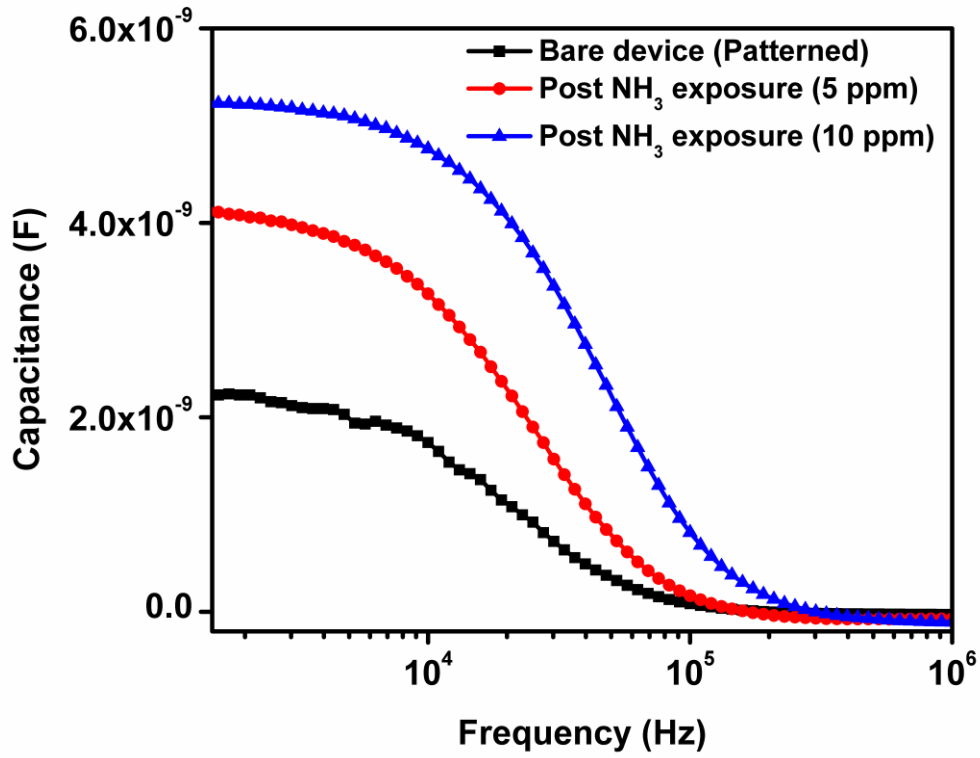


**Figure 5-11 C-f characteristics of a-Carbon/Silicon hetero-junction (patterned device) after exposure to different concentration of NH3**

C-V characteristics of patterned device for different concentrations of $NH_3$ exposure are shown in Figure 5-11. With increase in the target dose, the junction capacitance increases significantly. The change in capacitance of a patterned a-C/Si heterojunction can be explained by adsorption process, for an exposure dose of 5 ppm to patterned device, a change of 90 % ΔC was recorded. For an exposure dose of 10 ppm, a change of 141 % ΔC was recorded. Figure 5-12 shows the comparison in change ΔC between patterned device and unpatterned device with an ammonia exposure of 5 ppm with respect of base capacitance. Figure 5-13 shows the reliability analysis of the a-C/Si junction evaluated using 3 devices. As can be seen, the devices display almost identical C~f behaviour in the range of 1 KHz-1 MHz, with the peak capacitance at 1 KHz showing negligible variation.

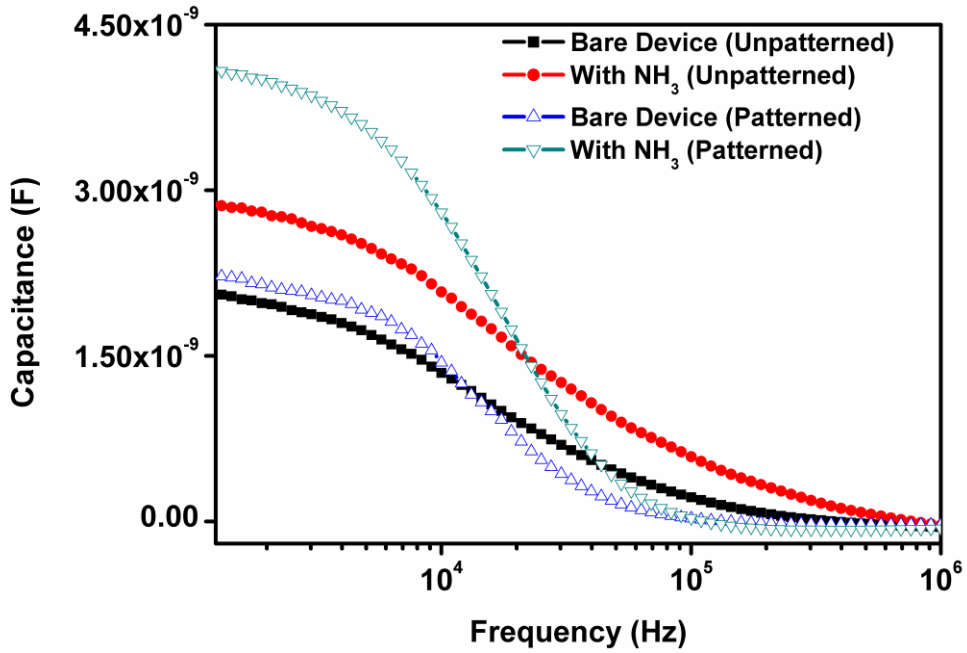


**Figure 5-12 Difference in change in Capacitance for patterned device and unpatterned device for an ammonia exposure of 5 ppm**

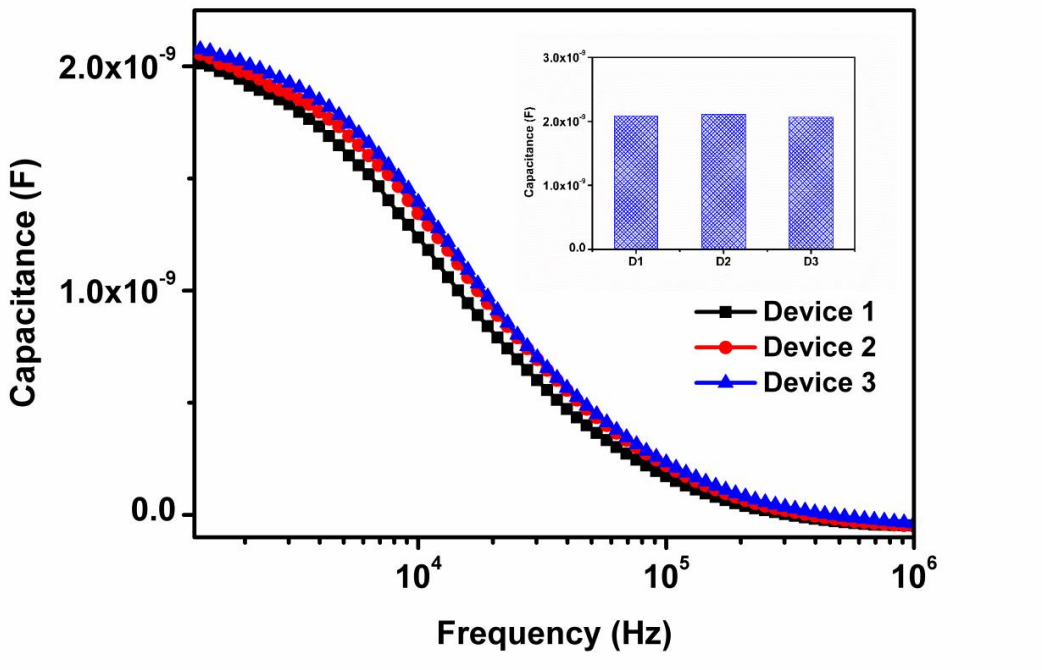


**Figure 5-13 Reliability analysis of the a-C/Si junction evaluated using 3 devices**

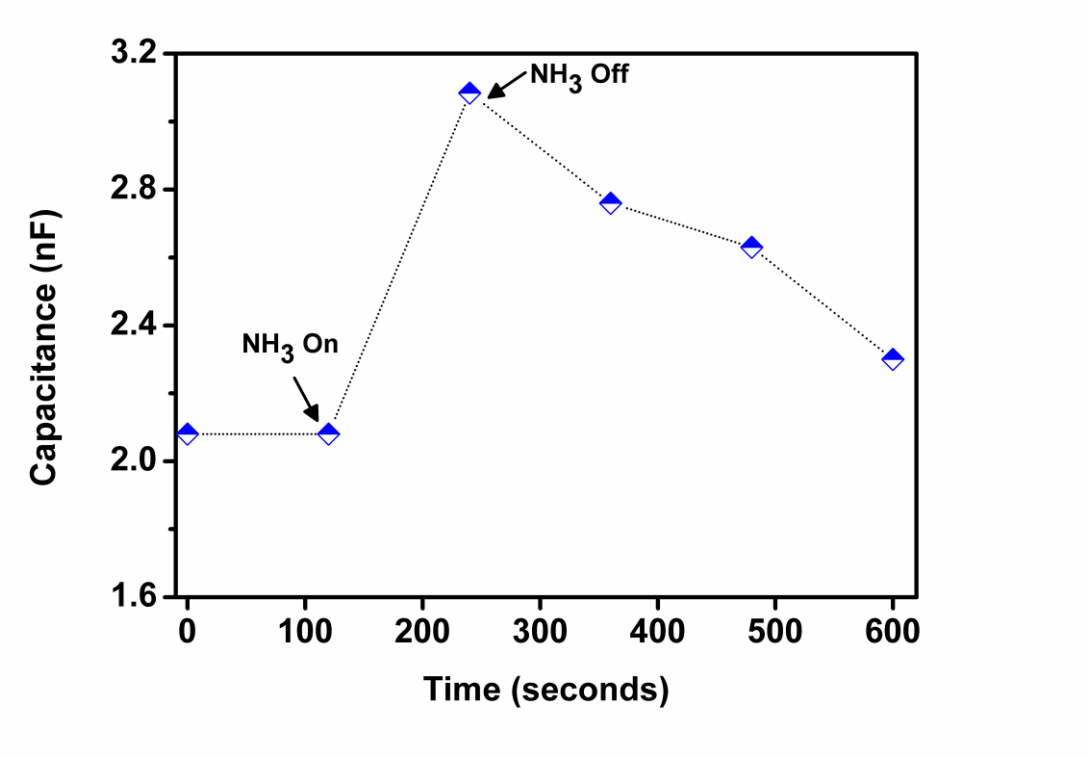


**Figure 5-14 $NH_3$ Turn On/Off Characteristics of device**

With respect to the detection of $NH_3$,as shown in Figure 5-14 we also monitored the response time and recovery time of the heterojunction devices. Here, the measurements of capacitance was carried out after every 120 seconds. The rise time of the device (from an unexposed condition to an exposed state) was found to be in the range of 5-10 sec (not interpretable from this graph), whereas the recovery time was found to be in range of 3-5 min at room temperature (for an exposure dose of 10 ppm). As can be seen, post ammonia exposure, when the device is placed in air, the desorption of $NH_3$ molecules take some time, which results in a recovery time ranging up to 5 minutes. We believe, further studies are essential in order that the recovery time is reduced to under 1 minute.

For an unpatterned device, we also calculated the limit of detection experimentally, and it was found to be 0.26 ppm. Note, this is in relation to an unpatterned device. By using a patterned device, we expect to enhance the same to a much lower value, as evidently, such a device provides better sensitivity to ammonia. However, such an analysis has not been included in this thesis work, and it will be addressed in future.

# Chapter 5

# Readout Circuit design for chemo resistive Sensor

## 6.1 Introduction

Today mobile phone has become an important and necessary gadget in everybody's life. We are using and miniaturizing the size of the principal devices for our comfort. We are now in a situation to use our smart phone as a power supply, data processing, and displaying device. Taking this into consideration, we can design readout circuits for sensors using mobile phone as a power supply device and data processing and displaying device. The micro USB of modern smart phones support OTG functionality which can be used as plug and play host. With a small circuit and using Arduino board we can measure capacitance, resistance, inductance etc. Since Sensors consume very less power we can derive power from mobile phones and we can use it for measurements of sensor. In this work, we have targeted such an application, wherein the readout circuit is aimed to be integrated with a chemiresistive sensor working in the range of few KΩ to hundreds of MΩ.

## 6.2 Block diagram

In this work, we have used Arduino board to sample the data from the sensor using 8-bit ADC present in ATMEGA 328 microcontroller and process the data using the microcontroller to the 16 * 2 LCD screen which is being powered by OTG port of mobile phone. Figure 6-1 shows the block diagram of the system and Figure 6-2 shows the circuit diagram using Arduino board.

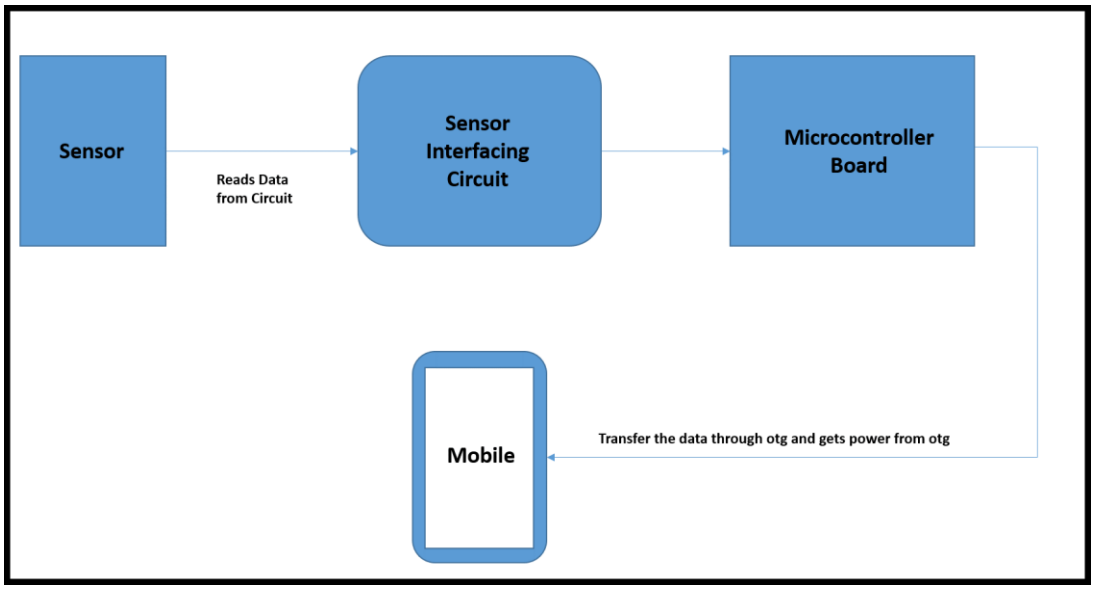


**Figure 6-1 Schematic representation of the block diagram showing sensor interfacing circuit , microcontroller board and Mobile**

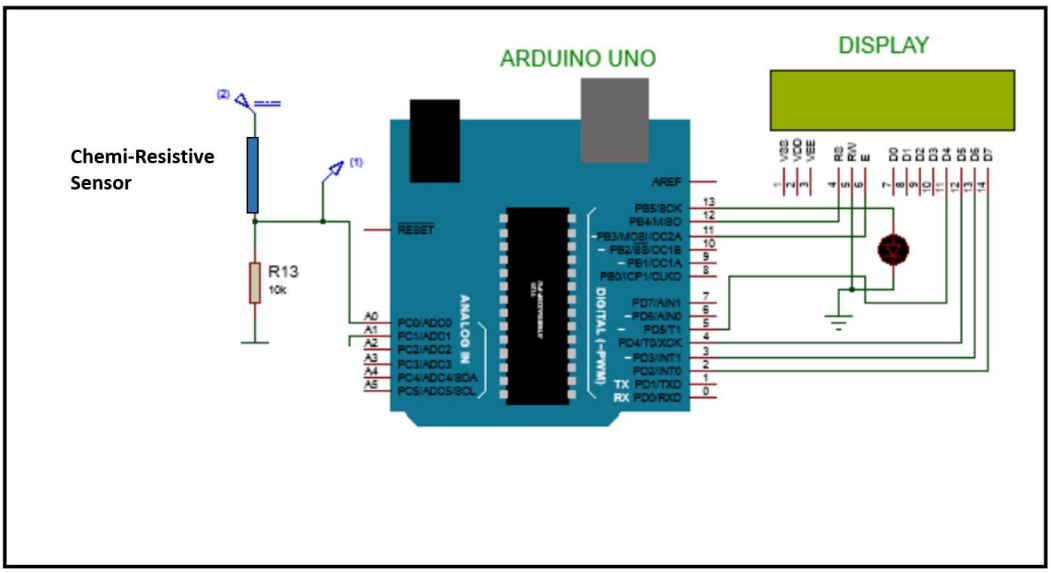


**Figure 6-2 Circuit diagram for readout circuit of chemo resistive sensor using 16 * 2 LCD display and Arduino uno microcontroller board**

## 6.3 Data Processing

The ATMEGA 328 is a powerful microcontroller to demonstrate various tasks. It is a low power consuming 10 bit microcontroller. This microcontroller has inbuilt 10 bit Analog to Digital Convertor for data sampling and acquisition. It will give us flexibility to have 1024 voltage levels. The ADC needs reference voltage for comparison. Here we are operating with 5 volts reference voltage which is coming from the mobile. After sampling the data from the sensor the data is converted into 10 bit digital data and then the raw data is processed with microcontroller and displayed on the JHD 16*2 display.

### 6.3.1 JHD LCD Display

This is a 16 *2 LCD display. It can print 16 letters in 2 rows. This display works with 5 v power supply. It can be operated with 8-bit data frame and 4-bit data frame. In this work this display is used in 8-bit data frame. It is shown in Figure 6-3

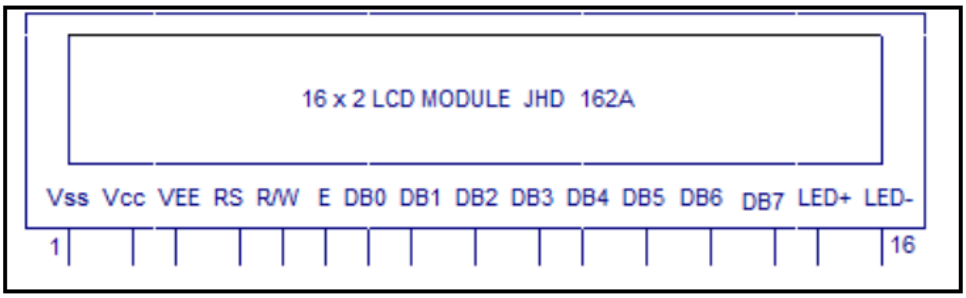


**Figure 6-3 JHD 16 *2 LCD Display pin configuration**

### 6.3.2 USB interfacing

In this work, power is drawn from micro USB port of mobile. Generally, the USB Type B has 5 pins for different purpose. Pins are shown in Figure 6-4 and description of micro USB pins are given in Table 2. We have to use the USB port as host. The mode of smartphone is defined by the ID pin in the port. The VCC pin form the port will act as the voltage supply for the IC. Data pins can be used to transfer the date to the mobile.

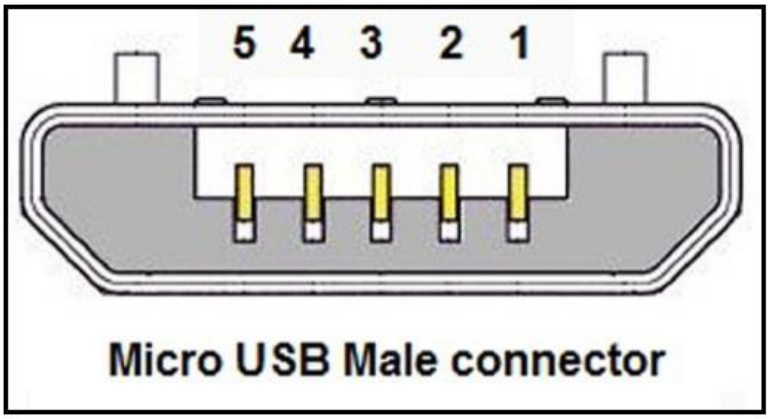


**Figure 6-4 Pins of USB connector**

| Pin | Name | Description |
|---|---|---|
| 1 | VCC | +5 VDC |
| 2 | D- | Data - |
| 3 | D+ | Data + |
| 4 | ID | Mode Detect |
| 5 | GND | Ground |

**Table 2 Pin description of micro USB**

## 6.4 Code and Algorithm for program

### 6.4.1 Code

Code is given in the APPENDIX 1.

### 6.4.2 Algorithm for the program

1. First initialize the lcd screen read and write pin, enable pin and 4 data pins and send the acknowledgment to the power supply.
2. Then begin serial port communication with 9600 bits per second.
3. Read the sensor data from input pin of ADC.
4. Convert the digital data into Analog voltage using the microcontroller after calibrating the sensor data.
5. Serially print the data on the display using the microcontroller
6. Then give a delay of 5 seconds and poll the sensor data and display it again in a loop manner.
7. Wait in loop till the analog data pin coming from the sensor.

## 6.5 Cadence Simulations and Results

Cadence is a virtual simulation platform which is used for simulation of circuits. It helps us to deal with real time operations. Apart from circuit designing, it gives us clear idea of various real time problems like noise, temperature and their effects. Following circuit is modelling of readout circuit design with ideal block is shown in Figure 6-5 and its result is shown in Figure 6-6

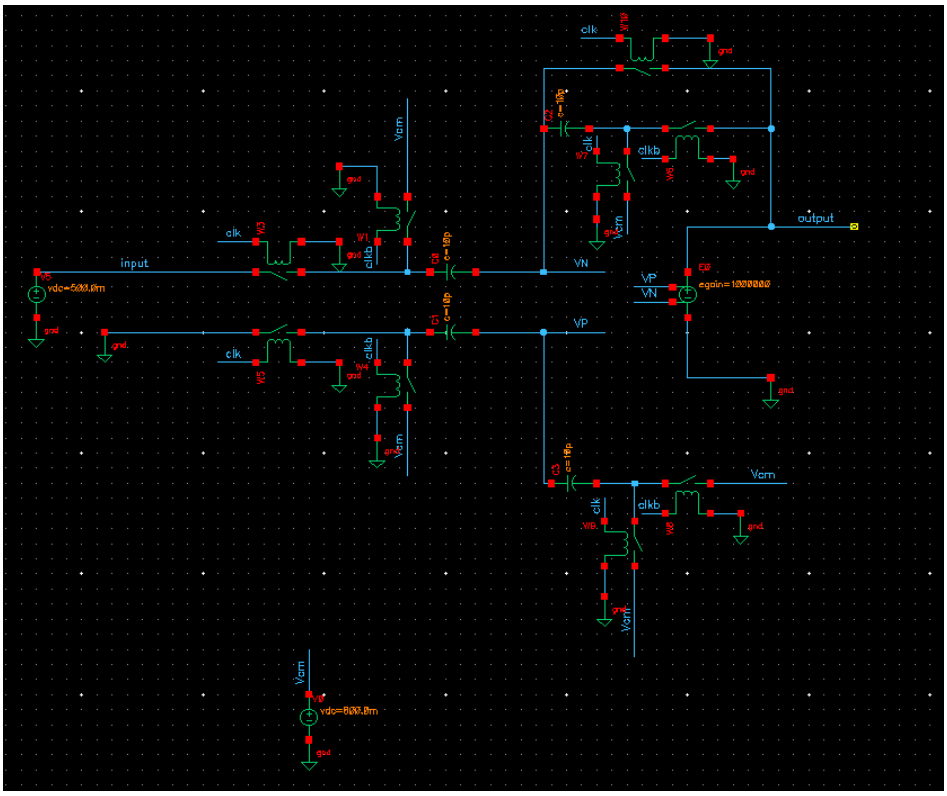


**Figure 6-5 Ideal modelling of Readout Circuit for Chemi-resistive Sensor**

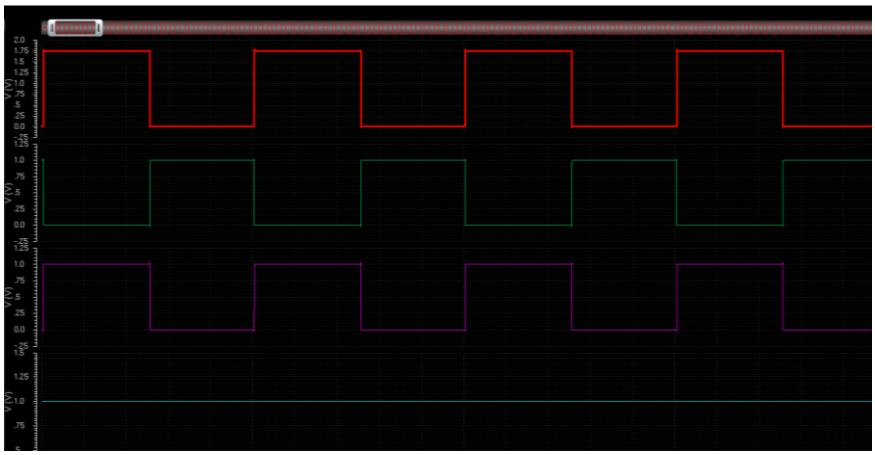

**Figure 6-6 Output Voltage of the ideally modelled circuit with input bias of 1 V**

Figure 6-7 and Figure 6-8 shows the op-amp design and switch design in cadence simulation tool.

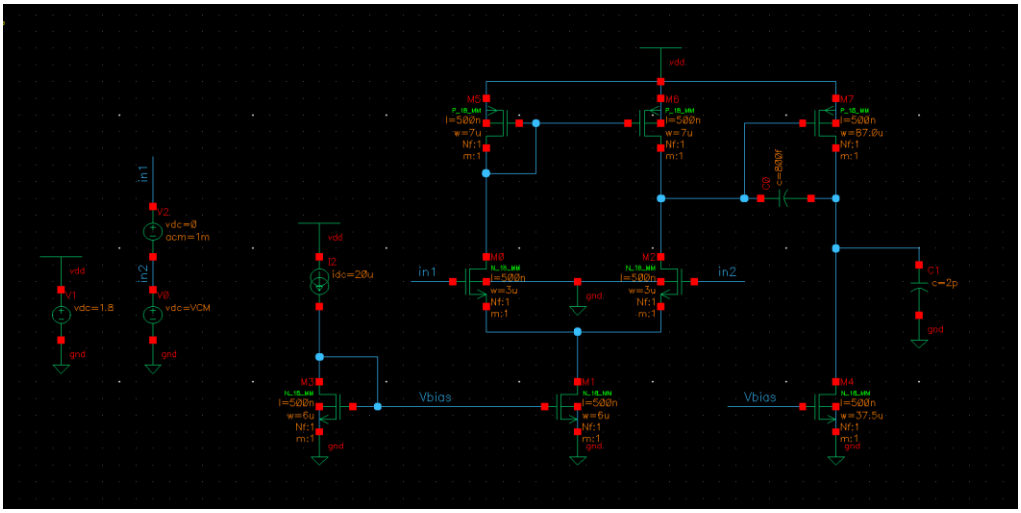


**Figure 6-7 Operational Amplifier Circuit diagram**

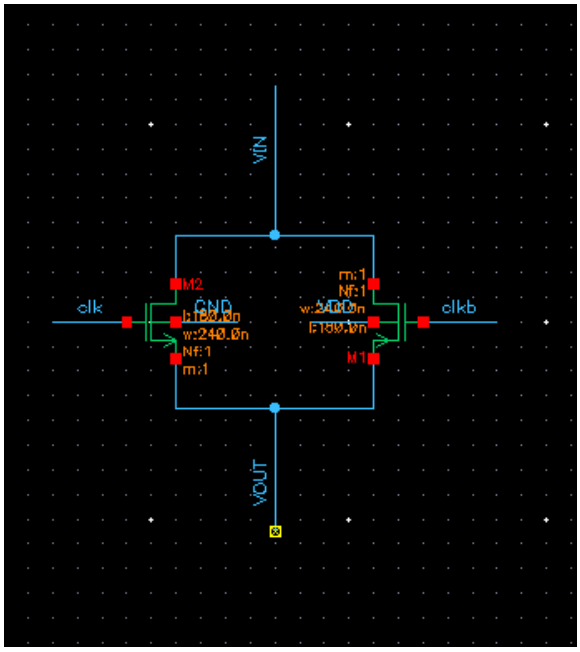


**Figure 6-8 Switch Circuit diagram**

Circuit modelling with ideal blocks has been done successfully. And one of the major blocks Operation Amplifier and Switch has been designed with 180nm node. All those simulations ran successfully. The idea explained and the circuit elaborated is tested.

# Chapter 6

# Summary and Further Work

## 7.1 Summary

In this M.Tech. thesis project, a room-temperature Ammonia ($NH_3$) sensor based on Amorphous-Carbon/Silicon(a-C/Si) heterojunction derived capacitive device has been developed, and a read-out circuit design for chemiresistive sensing is attempted. Herein, controlled pyrolysis of lithographically-patterned negative photoresist (SU8) thin-films has been performed to realize highly stable a-C/Si junctions. Use of pyrolysis is an economic way of realizing the carbon films as opposed to the conventional means of sputtering. Additionally, use of the photoresist allows us to preferably pattern the carbon film so as to develop heterojunction devices of varying shape and surface-area. In this study, we have explored the $NH_3$ sensing properties of an unpatterned a-C film based heterojunction, where, change in the capacitance-frequency (C~f) response of the heterojunction upon adsorption of $NH_3$ molecules on to the a-C surface is used as the transduction principle. The sensor accounts for a limit-of-detection of 0.26 ppm, a response-time of 5-10 sec, a post-exposure recovery time of 3-5 min and excellent selectivity, in addition to facilitating room temperature gas sensing.

We have also developed a Readout circuit to sense chemiresistive sensor. The system so developed will work with chemiresistive sensor platforms with target resistance ranging up to few MΩ. The requirement of the system was studied and the system was implemented. Ideal modelling of the complete system was done on cadence environment and simulations were ran successfully. A PCB based prototype of the system was prepared and tested.

## 7.2 Future work

In future, we intend to do a comprehensive study to determine the dependence of the device performance on several properties of the a-C film. Also, ammonia detection with patterned carbon structures is to be explored in much detail.

The current work on development of Readout circuit for chemiresistive sensors can be advanced to facilitate integration with mobile phones. A dedicated application can be developed which would help in data acquisition and display. A complete level system level design can be created using cadence layout editor, and the layout can subsequently be sent for fabrication. A chip level design can thus be developed which would enable standalone functioning of the envisaged system.

# Appendix I

```
#include <LiquidCrystal.h>

const int rs = 12, en = 11, d4 = 5, d5 = 4, d6 = 3, d7 = 2;

LiquidCrystal lcd(rs, en, d4, d5, d6, d7);

void setup()
{
 Serial.begin(9600);
}
void loop()
{
int sensorValue = analogRead(A0);
float voltage = sensorValue * (5.0 / 1023.0);
lcd.begin(16, 2);
lcd.print("voltage = ");
Serial.println(voltage);
lcd.print(voltage);
delay(10000);
}
```

# References


[1] Warneck, Peter. *Chemistry of the natural atmosphere*. vol. 71. Elsevier, 1999.

[2] Stercz, B., Perlstadt, H., Nagy, K. and Ongrádi, J., 2013. Immunochemistry of adenoviruses: limitations and new horizons of gene therapy. *Acta microbiologica et immunologica Hungarica*, *60*(4), pp.447-459.

[3] Henderson, R.K., Baker, A., Murphy, K.R., Hambly, A., Stuetz, R.M. and Khan, S.J., 2009. Fluorescence as a potential monitoring tool for recycled water systems: a review. *Water research*, *43*(4), pp.863-881.

[4] Spacek, L.A., Mudalel, M., Tittel, F., Risby, T.H. and Solga, S.F., 2015. Clinical utility of breath ammonia for evaluation of ammonia physiology in healthy and cirrhotic adults. *Journal of breath research*, *9*(4), p.047109.

[5] Kearney, D.J., Hubbard, T. and Putnam, D., 2002. Breath ammonia measurement in Helicobacter pylori infection. *Digestive diseases and sciences*, *47*(11), pp.2523-2530.

[6] Kamins, T., 1998. Structure. In *Polycrystalline Silicon for Integrated Circuits and Displays* (pp. 57-122). Springer, Boston, MA.

[7] Moos, R., Müller, R., Plog, C., Knezevic, A., Leye, H., Irion, E., Braun, T., Marquardt, K.J. and Binder, K., 2002. Selective ammonia exhaust gas sensor for automotive applications. *Sensors and Actuators B: Chemical*, *83*(1-3), pp.181-189.

[8] Dupré, P., 2001. Probing molecular species by cavity ringdown laser absorption spectroscopy, application to the spectroscopy and dynamics of jet-cooled NO2. *Comptes Rendus de l'Académie des Sciences-Series IV-Physics*, *2*(7), pp.929-964.

[9] Zakrzewska, K., 2001. Mixed oxides as gas sensors. *Thin solid films*, *391*(2), pp.229-238.

[10] Xu, J., Pan, Q. and Tian, Z., 2000. Grain size control and gas sensing properties of ZnO gas sensor. *Sensors and Actuators B: Chemical*, *66*(1-3), pp.277-279.

[11] Zhang, K., Wang, S., Malhotra, J., Hassler, J.R., Back, S.H., Wang, G., Chang, L., Xu, W., Miao, H., Leonardi, R. and Chen, Y.E., 2011. The unfolded protein response transducer IRE1α prevents ER stress-induced hepatic steatosis. *The EMBO journal*, *30*(7), pp.1357-1375.

[12] Arango, A.C., Johnson, L.R., Bliznyuk, V.N., Schlesinger, Z., Carter, S.A. and Hörhold, H.H., 2000. Efficient titanium oxide/conjugated polymer photovoltaics for solar energy conversion. *Advanced Materials*, *12*(22), pp.1689-1692.

[13] Huang, J., Virji, S., Weiller, B.H. and Kaner, R.B., 2003. Polyaniline nanofibers: facile synthesis and chemical sensors. *Journal of the American Chemical Society*, *125*(2), pp.314-315.

[14] Virji, S., Huang, J., Kaner, R.B. and Weiller, B.H., 2004. Polyaniline nanofiber gas sensors: examination of response mechanisms. *Nano letters*, *4*(3), pp.491-496

[15] Liu, J., Cao, Z. and Lu, Y., 2009. Functional nucleic acid sensors. *Chemical reviews*, *109*(5), pp.1948-1998.

[16] Mitzner, K.D., Sternhagen, J. and Galipeau, D.W., 2003. Development of a micromachined hazardous gas sensor array. *Sensors and Actuators B: Chemical*, *93*(1-3), pp.92-99.

[17] Llobet, E., Molas, G., Molinas, P., Calderer, J., Vilanova, X., Brezmes, J., Sueiras, J.E. and Correig, X., 2000. Fabrication of highly selective tungsten oxide ammonia sensors. *Journal of the Electrochemical Society*, *147*(2), pp.776-779.

[18] Li, P. and Li, X., 2006. A single-sided micromachined piezo resistive SiO2 cantilever sensor for ultra-sensitive detection of gaseous chemicals. *Journal of Micromechanics and Microengineering*, *16*(12), p.2539.

[19] Prasad, G.K., Radhakrishnan, T.P., Kumar, D.S. and Krishna, M.G., 2005. Ammonia sensing characteristics of thin film based on polyelectrolyte templated polyaniline. *Sensors and Actuators B: Chemical*, *106*(2), pp.626-631.

[20] Pandey, S., Goswami, G.K. and Nanda, K.K., 2013. Green synthesis of polysaccharide/gold nanoparticle nanocomposite: An efficient ammonia sensor. *Carbohydrate polymers*, *94*(1), pp.229-234

[21] Mariappan, R., Ponnuswamy, V., Suresh, R., Suresh, P., Bose, A.C. and Ragavendar, M., 2014. Role of substrate temperature on the properties of Na-doped ZnO thin film nanorods and performance of ammonia gas sensors using nebulizer spray pyrolysis technique. *Journal of Alloys and Compounds*, *582*, pp.387-391

[22] Pandey, S., Goswami, G.K. and Nanda, K.K., 2013. Green synthesis of polysaccharide/gold nanoparticle nanocomposite: An efficient ammonia sensor. *Carbohydrate polymers*, *94*(1), pp.229-234.

[23] Raju, A.R. and Rao, C.N.R., 1994. MoO3/TiO2 and Bi2MoO6 as ammonia sensors. *Sensors and Actuators B: Chemical*, *21*(1), pp.23-26.

[24] Roy, S.C., Sharma, G.L., Bhatnagar, M.C. and Samanta, S.B., 2005. Novel ammonia-sensing phenomena in sol–gel derived Ba0. 5Sr0. 5TiO3 thin films. *Sensors and Actuators B: Chemical*, *110*(2), pp.299-303.

[25] Rani, S., Roy, S.C., Puri, N.K., Bhatnagar, M.C. and Kanjilal, D., 2008. Enhancement of ammonia sensitivity in swift heavy ion irradiated nanocrystalline $SnO_2$ thin films. *Journal of Nanomaterials*, *2008*, p.69.

[26] Xue, Q., Chen, H., Li, Q., Yan, K., Besenbacher, F. and Dong, M., 2010. Room-temperature high-sensitivity detection of ammonia gas using the capacitance of carbon/silicon heterojunctions. *Energy & Environmental Science*, *3*(3), pp.288-291.

[27] Xue, Q., Chen, H., Li, Q., Yan, K., Besenbacher, F. and Dong, M., 2010. Room-temperature high-sensitivity detection of ammonia gas using the capacitance of carbon/silicon heterojunctions. *Energy & Environmental Science*, *3*(3), pp.288-291.

[28] E. Achenbach. Response of a solid oxide fuel cell to load change. J. Power Sources 57, (1995) 105–109

[29] http://www.electronics-tutorials.ws/opamp/op-amp-building-blocks.html

[30] ATmega328/P datasheet